

NTIS # PB2013-

SSC-468

**DEVELOPMENT OF A STRUCTURAL
HEALTH MONITORING PROTOTYPE
FOR SHIP STRUCTURES**



This document has been approved
For public release and sale; its
Distribution is unlimited

SHIP STRUCTURE COMMITTEE
2013

Ship Structure Committee

RDML J.A. Servidio
U. S. Coast Guard Assistant Commandant,
Assistant Commandant for Prevention Policy
Co-Chair, Ship Structure Committee

Mr. H. Paul Cojeen
Society of Naval Architects and Marine Engineers

Mr. Christopher McMahon
Director, Office of Ship Construction
Maritime Administration

Mr. Kevin Baetsen
Director of Engineering
Military Sealift Command

Mr. Jeffrey Lantz,
Commercial Regulations and Standards for the
Assistant Commandant for Marine Safety, Security
and Stewardship

Mr.
Deputy Assistant Commandant for Engineering and
Logistics

RADM Thomas Eccles
Chief Engineer and Deputy Commander
For Naval Systems Engineering (SEA05)
Co-Chair, Ship Structure Committee

Mr. Todd Grove
Chief Technical Officer (CTO)
American Bureau of Shipping

Ms. Julie Gascon
Director Design, Equipment and Boating Safety,
Marine Safety,
Transport Canada

Dr. Neil Pegg
Group Leader - Structural Mechanics
Defence Research & Development Canada - Atlantic

Mr. Eric C. Duncan
Director, Structural Integrity and Performance Division

Dr. John Pazik
Director, Ship Systems and Engineering Research
Division

SHIP STRUCTURE SUB-COMMITTEE

AMERICAN BUREAU OF SHIPPING (ABS)

Mr. Craig Bone
Mr. Phil Rynn
Mr. Tom Ingram

MARITIME ADMINISTRATION (MARAD)

Mr. Chao Lin
Mr. Richard Sonnenschein

NAVY/ONR / NAVSEA/ NSWCCD

Mr. David Qualley / Dr. Paul Hess
Mr. Erik Rasmussen / Dr. Roshdy Barsoum
Mr. Nat Nappi, Jr.
Mr. Dean Schleicher

UNITED STATES COAST GUARD

CAPT John Mauger
Mr. Jaideep Sirkar
Mr. Chris Cleary
Mr. Frank DeBord

DEFENCE RESEARCH & DEVELOPMENT CANADA

ATLANTIC

Mr. Malcolm Smith
Dr. Layton Gilroy

MILITARY SEALIFT COMMAND (MSC)

Mr. Michael W. Touma
Mr. Jitesh Kerai

TRANSPORT CANADA

Mr. Ian Campbell
Mr. Bashir Ahmed Golam
Mr. Luc Tremblay

SOCIETY OF NAVAL ARCHITECTS AND MARINE ENGINEERS (SNAME)

Mr. Rick Ashcroft
Mr. Dave Helgerson
Mr. Alex Landsburg
Mr. Paul H. Miller

Member Agencies:

*American Bureau of Shipping
Defence Research and Development Canada
Maritime Administration
Military Sealift Command
Naval Sea Systems Command
Office of Naval Research
Society of Naval Architects & Marine Engineers
Transport Canada
United States Coast Guard*



Address Correspondence to:

COMMANDANT (CG-ENG-2/SSC)
ATTN (EXECUTIVE DIRECTOR/SHIP
STRUCTURE COMMITTEE)
US COAST GUARD
2100 2ND ST SW STOP 7126
WASHINGTON DC 20593-7126
Website: <http://www.shipstructure.org>

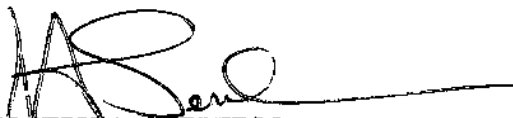
SSC – 468
SR – 1468


June 28, 2013

**DEVELOPMENT OF A STRUCTURAL HEALTH MONITORING PROTOTYPE FOR SHIP
STRUCTURES**

The complexity of many ship structures makes it difficult to analyze actual, in-use strength performance. Methods of detecting ship damage prior to being found by routine inspections could therefore provide a great benefit by both reducing maintenance costs and extending ship service life. Many other engineering disciplines, including civil, aerospace and mechanical engineering, have begun to incorporate structural health monitoring (SHM) into their designs in order to evaluate the real stresses induced in structures. SHM is an impedance-based method that utilizes piezoelectric transducers bonded to a structure in order to gain insight into the physical health of the object being monitored. Using real time algorithms and detection schemes and relying on the impedance analyzers to take SHM measurements, the goal of this research is to develop hardware specifically for naval applications. Successful experiments to validate the impedance method are conducted on a representative naval structure subjected to fatigue loading. Using the prototype SHM System, fatigue crack growth is detected, analyzed and compared with current structural inspection methods.

We thank the authors and Project Technical Committee for their dedication and research toward completing the objectives and tasks detailed throughout this paper and continuing the Ship Structure Committee's mission to enhance the safety of life at sea.


JOSEPH A. SERVIDIO
Rear Admiral, U.S. Coast Guard
Co-Chairman, Ship Structure Committee


T. J. ECCLES
Rear Admiral, U.S. Navy
Co-Chairman, Ship Structure Committee

1. Report No. 468	2. Government Accession No.	3. Recipient's Catalog No.	
4. Title and Subtitle Development of a Structural Health Monitoring Prototype for Ship Structures		5. Report Date	
		6. Performing Organization Code	
7. Author(s) Grisso, B.L.		8. Performing Organization Report No. SR-1468	
9. Performing Organization Name and Address Naval Surface Warfare Center, Carderock Division (NSWCCD) 9500 MacArthur Blvd West Bethesda, MD 20817		10. Work Unit No. (TRAIS)	
		11. Contract or Grant No. N0002412WX06200	
12. Sponsoring Agency Name and Address COMMANDANT (CG-ENG-2/SSC) ATTN (SHIP STRUCTURE COMMITTEE) US COAST GUARD 2100 2ND ST SW STOP 7126 WASHINGTON DC 20593-7126		13. Type of Report Final Report	
		14. Sponsoring Agency Code CG - 5P	
15. Supplementary Notes The research completed by the above author for the Ship Structure Committee was reviewed by the Project Technical Committee for satisfactory completion of the objectives outlined in the Statement of Work developed and approved for funding by the Principal Members of the Ship Structure Committee. Sponsored by the Ship Structure Committee and its member agencies			
16. Abstract Impedance-based structural health monitoring (SHM) utilizes piezoelectric transducers bonded to a structure in order to gain insight into the physical health of the object being monitored. By observing the electrical impedance of the piezoelectric transducer, changes to the structure can be identified. Typical impedance SHM measurements rely upon impedance analyzers or other complex hardware. Research presented in this report focuses on developing impedance hardware specifically for naval applications. Before a prototype is developed, the functionality of impedance SHM is verified on a representative naval structure. A welded aluminum specimen is subjected to fatigue loading, and the impedance method is used to successfully detect fatigue crack growth. Components of an impedance SHM prototype are then considered for inclusion in the hardware and are validated on an aluminum test specimen. Finally, an initial prototype is designed based upon an impedance integrated circuit.			
17. Key Words structural health monitoring, Damage Detection, Impedance Method		18. Distribution Statement National Technical Information Service U.S. Department of Commerce Springfield, VA 22151 Ph. (703) 487-4650 / www.ntis.gov	
19. Security Classif. (of this report) Unclassified	20. Security Classif. (of this page) Unclassified	21. No. of Pages	22. Price

Technical Report Documentation Page

1. Report No.	2. Government Accession No.	3. Recipient's Catalog No.	
4. Title and Subtitle Development of a Structural Health Monitoring Prototype for Ship Structures		5. Report Date December 2012	
		6. Performing Organization Code	
7. Author(s) Grisso, B. L.		8. Performing Organization Report No. SR-1468	
9. Performing Organization Name and Address Naval Surface Warfare Center, Carderock Division 9500 MacArthur Blvd West Bethesda, MD 20817		10. Work Unit No. (TRAIS)	
		11. Contract or Grant No. N0002412WX06200	
12. Sponsoring Agency Name and Address Ship Structure Committee, U. S. Coast Guard (G-MSE/SSC) 2100 Second Street, SW Washington, D.C. 20593-0001		13. Type of Report and Period Covered Final Report 4/11-12/12	
		14. Sponsoring Agency Code G-M	
15. Supplementary Notes Sponsored by the Ship Structure Committee. Jointly funded by its member agencies			
16. Abstract Impedance-based structural health monitoring (SHM) utilizes piezoelectric transducers bonded to a structure in order to gain insight into the physical health of the object being monitored. By observing the electrical impedance of the piezoelectric transducer, changes to the structure can be identified. Typical impedance SHM measurements rely upon impedance analyzers or other complex hardware. Research presented in this report focuses on developing impedance hardware specifically for naval applications. Before a prototype is developed, the functionality of impedance SHM is verified on a representative naval structure. A welded aluminum specimen is subjected to fatigue loading, and the impedance method is used to successfully detect fatigue crack growth. Components of an impedance SHM prototype are then considered for inclusion in the hardware and are validated on an aluminum test specimen. Finally, an initial prototype is designed based upon an impedance integrated circuit.			
17. Key Words Structural Health Monitoring, Damage Detection, Impedance Method		18. Distribution Statement DISTRIBUTION STATEMENT A. Approved for public release; distribution is unlimited. Available from: National Technical Information Service Springfield, VA 22161 (703) 487-4650	
19. Security Classif. (of this report) Unclassified	20. Security Classif. (of this page) Unclassified	21. No. of Pages	22. Price

CONVERSION FACTORS
(Approximate conversions to metric measures)

To convert from	to	Function	Value
LENGTH			
inches	meters	divide	39.3701
inches	millimeters	multiply by	25.4000
feet	meters	divide by	3.2808
VOLUME			
cubic feet	cubic meters	divide by	35.3149
cubic inches	cubic meters	divide by	61,024
SECTION MODULUS			
inches ² feet ²	centimeters ² meters ²	multiply by	1.9665
inches ² feet ²	centimeters ³	multiply by	196.6448
inches ⁴	centimeters ³	multiply by	16.3871
MOMENT OF INERTIA			
inches ² feet ²	centimeters ² meters	divide by	1.6684
inches ² feet ²	centimeters ⁴	multiply by	5993.73
inches ⁴	centimeters ⁴	multiply by	41.623
FORCE OR MASS			
long tons	tonne	multiply by	1.0160
long tons	kilograms	multiply by	1016.047
pounds	tonnes	divide by	2204.62
pounds	kilograms	divide by	2.2046
pounds	Newtons	multiply by	4.4482
PRESSURE OR STRESS			
pounds/inch ²	Newtons/meter ² (Pascals)	multiply by	6894.757
kilo pounds/inch ²	mega Newtons/meter ² (mega Pascals)	multiply by	6.8947
BENDING OR TORQUE			
foot tons	meter tons	divide by	3.2291
foot pounds	kilogram meters	divide by	7.23285
foot pounds	Newton meters	multiply by	1.35582
ENERGY			
foot pounds	Joules	multiply by	1.355826
STRESS INTENSITY			
kilo pound/inch ² inch ^{1/2} (ksi ^{1/2} /in)	mega Newton MNm ^{3/2}	multiply by	1.0998
J-INTEGRAL			
kilo pound/inch	Joules/mm ²	multiply by	0.1753
kilo pound/inch	kilo Joules/m ²	multiply by	175.3

Table of Contents

1. Introduction	1
1.1 SHM Motivation for Naval Applications.....	2
1.2 Impedance-based SHM	3
1.3 Impedance Specific Hardware	4
1.3.1 Low-cost Impedance Circuit.....	4
1.3.2 Impedance Integrated Circuit	6
1.4 Overview of Research	8
1.4.1 Research Goals	8
1.4.2 Chapter Summaries	9
2. Impedance Health Monitoring of an Aluminum Fatigue Specimen.....	10
2.1 Component Fabrication	11
2.2 Fatigue Testing and Data Acquisition	11
2.3 Data Analysis.....	15
3. Hardware Development.....	23
3.1 Basic Evaluation Board Operation.....	23
3.2 Evaluation Board Piezoelectric Testing	25
3.3 Evaluation Board Modifications.....	29
3.4 Modified Board Health Monitoring Testing.....	30
4. Initial Prototype Design	41
4.1 Low Ohm Impedance Measurements	41
4.2 Prototype Concept.....	45
4.2.1 Design and Verification Process	45

4.2.2 Initial Design.....	46
5. Conclusions and Recommendations.....	49
5.1 Brief Report Summary	49
5.2 Contributions.....	50
5.3 Future Work Recommendations	50
Acknowledgements	51
References.....	52

List of Figures

Figure 1. The front of an identical fatigue specimen is shown, and the four piezoelectric discs bonded to the plate are labeled.....	13
Figure 2. The butt weld and rathole where crack initiation occurs are displayed.....	13
Figure 3. The crack growth is displayed on the back of the main plate. Note that the total, not random amplitude, cycle count is used in the markings.	14
Figure 4. Real impedance is displayed for Piezo 1 from 100 – 200 kHz.	16
Figure 5. The RMSD damage metric displays the amount of change in each impedance signature to the first baseline measurement.....	16
Figure 6. The real impedance is displayed for Piezo 1 from 170 – 200 kHz.....	17
Figure 7. The RMSD damage metric values are shown for Piezo 1 from 170 – 200 kHz.	18
Figure 8. The real impedance is show for Piezo 2 from 170 – 200 kHz.	20
Figure 9. The RMSD damage metric values are shown for Piezo 2 from 170 – 200 kHz.	21
Figure 10. The real impedance (top) and RMSD damage metric values (bottom) are shown for Piezo 3 from 170 – 200 kHz.....	22
Figure 11. The AD5933 evaluation board.....	24
Figure 12. A 15pF capacitor is measured with the AD5933 evaluation board.....	25
Figure 13. A small plate with a butt weld and three piezo discs is shown.	26
Figure 14. Impedance magnitude is shown as measured with the HP 4194A impedance analyzer from 10 – 41.98 kHz.....	27
Figure 15. Impedance magnitude is shown as measured with the HP 4194A impedance analyzer from 35 – 36 kHz.....	27
Figure 16. The test plate is connected to the AD5933 EB and controlled via a USB laptop connection.	28

Figure 17. A comparison of HP 4914A and AD5933 impedance magnitude data from 35 – 36 kHz.	29
Figure 18. The modified evaluation board (left) is shown with a view of the amplifier (right)	30
Figure 19. The base plate of the test structure. Dimensions are in inches unless otherwise specified.	32
Figure 20. The dimensions (in inches) are shown for a plate doubler.	33
Figure 21. The base plate is placed in end clamps to supply fixed-fixed boundary conditions. The HP 4194A impedance analyzer is shown in the right of the picture.....	33
Figure 22. The left doubler, piezo disc, and loosened bolt labels are displayed.....	34
Figure 23. The real impedance (top) and RMSD damage metric (bottom) are shown from 10 – 41.98 kHz as measured by the HP 4194A impedance analyzer. 35	
Figure 24. The real impedance (top) and RMSD damage metric (bottom) are shown from 20 – 30 kHz as measured by the HP 4194A impedance analyzer.....	36
Figure 25. The real impedance (top) and RMSD damage metric (bottom) are shown from 10 – 41.98 kHz as measured by the AD5933 evaluation board.....	37
Figure 26. The real impedance (top) and RMSD damage metric (bottom) are shown from 20 – 30 kHz as measured by the AD5933 evaluation board.	38
Figure 27. One baseline measurement is show for both the AD5933 evaluation board and the HP 4914A impedance analyzer from 10 – 41.98 kHz.	39
Figure 28. One baseline measurement is shown for both the AD5933 evaluation board and the HP 4914A impedance analyzer from 20 – 30 kHz.	40
Figure 29. The Analog Devices CN0217 evaluation board.....	42
Figure 30. Real impedance signatures acquired from the CN0217 evaluation board and HP 4194A impedance analyzer are compared from 10 – 41.98 kHz.	43
Figure 31. Real impedance signatures acquired from the CN0217 evaluation board and HP 4194A impedance analyzer are compared from 30 – 35 kHz.....	44
Figure 32. Real impedance signatures acquired from the CN0217 evaluation board and HP 4194A impedance analyzer are compared from 25 – 27 kHz.	45

Figure 33. An initial circuit block diagram is shown based upon the AD5933 chip and CN0217 circuit. 46

List of Tables

Table 1. Measurement and damage condition descriptions.	14
--	----

1. Introduction

Ship structures are highly complex, often consisting of a mixture of different building materials (steel alloys, aluminum alloys, composites, etc.), manufacturing processes (extrusions, plate rolling, etc.), and assembly methods (welding, bolted connections, etc.). Newer ships may even consist of non-conventional hull forms which add to the complexity of understanding how the ship will perform over its entire service life. Unquantified loading on ships further extends the uncertainty of predicting future performance. Besides typical cyclic loads leading to fatigue failure, ships can often be subject to loading events (*i.e.* wave slam events) which exceed designed load limits or were unaccounted for in fatigue analyses. With all of these uncertainties, as well as the possibility of manufacturing defects and errors or material flaws, the possibility exists for a ship to experience damage (cracking, corrosion, etc.) long before any predictive technique would indicate. Methods of detecting ship damage prior to being found by routine inspections could therefore provide a great benefit by both reducing maintenance costs and extending ship service life.

For any number of structures, including civil, aerospace, and mechanical engineering infrastructure, structural health monitoring (SHM) is the process of implementing a damage identification strategy (Farrar and Worden 2007). As opposed to the way one might think about the use of traditional nondestructive evaluation (NDE) techniques such as liquid penetrant inspection, magnetic inspection, eddy-current inspection, radiography, or ultrasonic inspection to detect damage (Doherty 1987), SHM methods are commonly performed while the structure is in use (Inman *et al.* 2005). While NDE techniques generally require the system of interest to be inoperable, SHM can often be done in real time with algorithms and detection schemes finding changes to the structure almost instantaneously.

The obvious goal of any health monitoring application is to detect changes, or damage, to the underlying structure. Damage to typical monitored structures is defined as any changes to the material, system geometric properties, boundary conditions, or system connectivity which are either intentionally or unintentionally brought about.

Usually, to be considered damage, these changes must adversely affect the current or future performance of the system (Doebbling *et al.* 1998, Inman *et al.* 2005, Farrar and Worden 2007).

Adams (2007) expands the definition of health monitoring to identifying four characteristics of a structure as it operates:

1. the operational and environmental loads acting on a structure,
2. the mechanical damage caused by these loads,
3. the growth of this damage during operation, and
4. the future performance of the structure as due to cumulative damage effects.

Many ships, both naval and commercial, are now being equipped with temporary or permanent hull monitoring systems (ABS 2003, Salvino and Brady 2007). These hull monitoring systems would theoretically do an effective job of determining the operational and environmental loads necessary for SHM defined in Step 1 by Adams (2007). The focus of research in this report is to concentrate on technologies which will characterize Steps 2 and 3 to detect, characterize, and track the growth of damage in ship structures. Combining the knowledge gained in the first three steps of health monitoring with ship design criteria, modeling, and operational characteristics could lead to Step 4, which accurately predicts the future performance of a ship.

1.1 SHM Motivation for Naval Applications

The US Navy has recently been incorporating non-traditional construction materials, namely aluminum and composites, into ship structures with greater frequency (Hess 2007). Obvious advantages to these materials include properties such as strength-to-weight ratio and corrosion resistance, which allow for both high speed and specialized performance ships. However, the long term operational maintainability of these materials remains largely unknown.

Understanding the long-term performance of lightweight material usage in advance ship designs would traditionally involve either extensive testing or intensive inspection and maintenance. Large experimental programs prior to ship fabrication with

extensive material, component, and structure testing result in delays to ship production and, ultimately, a lack of desired ship usage for the fleet. Frequent inspection and maintenance routines applied to abate any early onset damage also reduce operational ship availability. As such, both traditional options come with heavy financial obligations.

Structural health monitoring is one of the techniques proposed to bridge the gap between extensive testing and frequent inspections and maintenance. Real-time monitoring of ships loads could not only influence maintenance decisions but current operation decisions as well (Hess 2007). Damage detection systems deployed in difficult to access areas could greatly improve the time and cost required for routine maintenance. Furthermore, consistent and long-term health monitoring can influence life-cycle decisions regarding end-of-service or useful life calculations. Impedance-based SHM is just one of the many techniques being investigated for use in naval applications to enhance ship and crew safety and reduce the total ownership costs of ship and ship systems to the Navy (Salvino and Brady 2007).

1.2 Impedance-based SHM

Impedance-based structural health monitoring techniques utilize small, self-sensing piezoelectric patches bonded to a structure to both simultaneously excite the structure with high-frequency excitations as well as monitor changes in the patch electrical impedance signature (Park and Inman 2007). Since the piezoelectric is attached directly to the structure of interest, it has been shown that the mechanical impedance of the structure is directly correlated with the electrical impedance of the patch (Liang *et al.* 1994a, 1994b). Thus, by observing the electrical impedance of the piezoelectric, assessments can be made about the integrity of the mechanical structure.

Using the impedance method, damage has been successfully detected on a variety of structures from simple beams and plates to bridge truss structures, airplane composite patch repairs, and pipeline structures (Park *et al.* 2003). Several damage mechanisms have been proven detectable, including cracking, bolt loosening, composite delaminations, and more.

Traditionally, the impedance method requires the use of an impedance analyzer, which is used to measure and analyze impedance in electrical components and systems. Impedance analyzers generally provide precise electrical impedance (as well as capacitance, inductance, resistance, etc.) measurements over broad frequency ranges with extensive functionality and display options. Due to their high performance intended for electronics quality control, design, and other tasks, such analyzers are often bulky, expensive, and not suited for permanent placement on a structure. For these reasons, many research investigations in the past decade have focused on hardware specifically designed to perform impedance-based SHM.

1.3 Impedance Specific Hardware

The following literature review is by no means intended to be all inclusive of developed impedance SHM hardware. Although many of the significant works are cited, other sources (Grisso 2007) have covered many of the initial development of impedance hardware in greater detail, and a new comprehensive review paper on impedance method hardware is expected in the near future. The works cited here are intended to give a general overview of some of the research which has been completed in the area of hardware or techniques development for the impedance method.

1.3.1 Low-cost Impedance Circuit

As mentioned in Section 1.2, an impedance analyzer is traditionally required to obtain impedance SHM data. While using an analyzer is generally a convenient, precise acquisition device for laboratories, the cost and size of impedance analyzers is typically impractical for field or permanently deployed settings. To get around using an impedance analyzer, the low cost impedance technique can be used (Peairs *et al.* 2004). The low cost circuit is simply a voltage divider consisting of a sensing resistor and capacitor in series with the transducer under test. The output voltage across the sensing resistor and capacitor is proportional to the current through the whole circuit. By measuring the voltage across the equivalent sensing circuit with a FFT analyzer, impedance can be accurately approximated by calculating the ratio of the applied function generator voltage and resulting sensing circuit voltage.

Since Peairs developed the low cost circuit (2004), others have looked to reduce the cost of necessary measurement components even further. While a FFT analyzer may cost up to \$10,000, other laboratory equipment may be less expensive and more convenient. Bhalla *et al.* (2009) were able to take absolute admittance (inverse of impedance) measurements utilizing basic equipment such as a function generator and digital multimeter. In a laboratory setting, the non-complex measurements were shown to effectively detect drilled hole damage in an aluminum beam. Results compared favorably to measurements taken with traditional (impedance analyzer or LCR meter) equipment. This work was then extended further by using an oscilloscope in place of the multimeter to monitor the piezoelectric (Panigrahi *et al.* 2010).

Another approach has been to develop more compact hardware with functionality specific to SHM (as opposed to generic measurement devices). These devices might not only acquire data, but could also instantaneously analyze the data and distribute calculated results. The MEMS-Augmented Structural Sensor (MASSpatch) was the first device to autonomously perform impedance SHM by incorporating on-board computing and wireless transmissions (Grisso 2004, Grisso *et al.* 2005). The device could interrogate a structure utilizing the low cost impedance method, and all the structural interrogation and data analysis is performed in near real time at the sensor location. Wireless transmissions alert the end user to any harmful changes in the structure.

Extending upon this research, more advanced systems developed from the low cost circuit relied on a digital signal processor (DSP) platform (Grisso 2007, Kim *et al.* 2007a, Grisso and Inman 2008). A completely digital prototype is used to minimize power consumption (Kim *et al.* 2007b). By utilizing a wideband excitation technique, the system power was even further reduced and excitation time decreased (Kim *et al.* 2007c).

Completely autonomous hardware is achieved via a battery and thermoelectric power harvesting (Grisso 2007, Grisso *et al.* 2007) and by harvesting structural vibrations (Zhou *et al.* 2010a). Based upon the all-digital platform, additional capabilities have been developed including combining impedance with Lamb wave SHM, automated damage mitigation (Kim *et al.* 2009), and the incorporation of digital sensor diagnostics for the detection transducer disbonds or breakage (Grisso *et al.*

2008). An ultra-low power device, including temperature compensation, has also been fabricated (Zhou *et al.* 2010b).

Giurgiutiu and Xu (2004) designed and tested a field portable impedance measurement device using standard laboratory equipment. A PC operating a LabVIEW program is connected to a function generator through a GPIB card. The function generator excites the structure being tested, and a PCI DAQ card records the excitation signal and structural response. Both signals are fed into the LabVIEW program for analysis. To circumvent the necessity of converting temporal measurements to the frequency domain, Xu and Giurgiutiu (2006) developed a digital signal processor (DSP) based impedance analyzer system. A transfer function method for taking impedance measurements is implemented to improve time efficiency and implementation ease for field use.

To avoid the use of off-the-shelf components, which may typically have more functionality and additional circuitry than required for SHM-specific applications, Wang *et al.* (2010) developed their own integrated circuit for impedance SHM. By incorporating components such as a digitally-controlled oscillator for actuation, a peak detector for sensing, and digital-to-analog converter, a circuit was designed specifically to automatically acquire impedance measurements in a typical SHM frequency band (7.5 kHz to 277 kHz). Numerical simulations of the circuit determined a power consumption of only 18.15 mW. When fabricated, the circuit could be incorporated with other components such as power sources and wireless communication for a complete data acquisition device.

1.3.2 Impedance Integrated Circuit

A secondary approach to obtaining low-power, portable impedance SHM measurements arose with the introduction of an impedance measurement integrated circuit (IC) developed by Analog Devices, Inc. Two impedance ICs were released, the AD5933 and AD5934. While neither IC was developed specifically with health monitoring measurements utilizing piezoelectric transducers in mind, the AD5933 is the more suitable choice for impedance-based methods due to its higher sampling speed (and thus higher frequency bandwidth). Either IC allows for the direct measurement of

impedance without the use of a low cost circuit. Both impedance chips also come in an evaluation board package to assist in determining the chip functionality and performance characteristics.

Researches at Los Alamos National Laboratory were some of the first to develop components around the AD5933 for impedance SHM purposes. Their first solution, the Wireless Impedance Device 1 (WID 1) used a microprocessor to control the AD5933 evaluation board (Mascarenas *et al.* 2006). Xbee radios were used to wirelessly transmit the acquired impedance signatures.

With the introduction of the WID 1.5, the AD5933 impedance chip was incorporated into a custom printed circuit board (PCB) design (Overly *et al.* 2007a). The WID 2.0 upgrades the microcontroller used to operate the AD5933, and two multiplexers are included to allow the system to measure up to seven different sensors (Overly *et al.* 2007b). Both units use radios to wirelessly transmit data which is then processed offline. WID 3 introduced low frequency analog-to-digital (ADC) and digital-to-analog (DAC) converters to the hardware allowing for the acquisition of structural modal properties via accelerometer measurements (Taylor *et al.* 2010).

Similar to the WID 1, others have also modified the AD5933 evaluation board for use with detecting damage. Park *et al.* (2007) modified the AD5933 evaluation board for use in detecting corrosion of an aluminum beam with a composite piezoelectric transducer. Park *et al.* (2009) then developed their own wireless impedance sensor node with multiplexers and components similar to WID 2.0. Min *et al.* (2010) improved the sensor node by adding the ability for solar powered operation via battery recharging, sensors and algorithms for temperature compensation and sensor diagnostics, and improved wireless communication for networking. Recently, Quinn *et al.* (2011, 2012) investigated the use of adding the AD5933 to embeddable wireless sensor node placed into wet concrete to monitor both the concrete cure and long-term structural condition.

1.4 Overview of Research

1.4.1 Research Goals

As highlighted in the above literature review, there is an active research community dedicated to the development of compact, autonomous hardware to simplify the implementation of impedance-based health monitoring. While many of the resulting hardware designs and prototypes are quite advanced, they are still only in the prototype and laboratory verification stage. The major drawback of prototype systems for government or of commercial applications is that none of these devices are available to purchase for further research investigations or implementation directly into structures. Many devices are likely not adaptable to very specific application needs. In the case of designing hardware for use with Navy ships and ship systems, the devices must conform to open architecture standards, which is a feature typically not considered in many designs.

Some ship platforms, such as the Littoral Combat Ships, are incorporating the use of open architecture for ship systems to reduce overall acquisition costs and increase the transition speed of new technologies to the ship. As opposed to a closed system where a design cannot be readily changed, an open system is easily updateable through third party development, has extensive documentation, and utilizes standard interfaces. While open architecture is not a requirement for all ship systems, following the best practices for open architecture could potentially help system acceptance and integration. In this research, standard components and interfaces will be exploited whenever possible.

Based on these limitations and concerns, the motivation for impedance hardware specifically for ship structures is clear. The goal of this research is to begin the development of SHM hardware specifically designed for naval applications. Specifications necessary for ship deployment will be considered early in prototype development. Research here is not intended to be as advanced as some of the impedance hardware already developed, but rather to design an initial piece of hardware as a basis for further development while incorporating naval specific needs and regulations (open architecture, etc.) throughout the process. Future modifications

can then begin to employ the advanced features of other system. Eventually, the prototype unit will be capable of operating on ship power or independently through a battery or capacitor. Energy harvesting methodologies could then even be deployed for remote or limited access regions.

1.4.2 Chapter Summaries

In the following chapters, investigations from a number of different research topics will be presented. The overarching goal each of these chapters leads to is impedance SHM hardware suitable for naval or marine applications. Results from each chapter typically build on preceding studies.

Chapter Two presents the application of impedance-based techniques for detecting damage in a structure undergoing cyclic fatigue loading. The aluminum test specimen used in this chapter incorporates typical details used in naval shipbuilding. Results indicate that impedance techniques are appropriate for early detection of fatigue damage in specimen flaws.

The first efforts in understanding an impedance measurement integrated circuit are outlined in Chapter Three. First, the basic functions of a chip on an evaluation board are outlined. Once basic operations are well understood, impedance health monitoring investigations are undertaken on a specimen representative of a component found in ships. Results compared favorably with those from an impedance analyzer.

In Chapter Four, the initial steps at impedance hardware development are outlined. A promising new hardware improvement is evaluated for potential use in the prototype circuit design. Initial block diagram and software development details are then revealed. Chapter Five wraps up the report with a brief outline, a list of research contributions, and recommendations for appropriate future work.

2. Impedance Health Monitoring of an Aluminum Fatigue Specimen

Recently, the use of aluminum has been incorporated into the design and fabrication of marine and naval vessels with increasing regularity. Many of the naval applications for aluminum include high speed and high performance vessels. While aluminum is a natural material choice for these ships due to its lightweight properties, the use of aluminum comes with several challenges including limited performance knowledge of the materials, aluminum sensitization, structural fatigue performance, and strength of welded aluminum structures. With these challenging areas, the desire for a comprehensive naval structural health monitoring system has been an area of great interest (Hess 2007, Swartz *et al.* 2010, Grisso *et al.* 2011a, Grisso *et al.* 2011b).

One area of concern in aluminum structures is the heat-affected zone (HAZ) generated as a result of the aluminum welding process (Kou 2003, Shankar and Wu 2002). Unlike welding in steel, where nearly all tensile strength is retained, welding in aluminum can leave localized weakness in the base material near the weld, known as the heat-affected zone, due to heat generated from welding. In some aluminum alloys, up to a 50% reduction in tensile strength is possible due to the HAZ. Despite these major differences between steel and aluminum, most current structural analysis and design procedures of an aluminum ship are still based on data and knowledge of designing a steel ship. As a result, the welds and surrounding HAZ can act as crack initiation sites due to operational cyclic loading.

In this chapter, a representative welded aluminum test specimen is monitored via the impedance method for structural health monitoring while undergoing cyclic fatigue loading. As noted in the introduction, the impedance technique has been utilized as a highly effective SHM technique for a variety of structures. Advantages include the ability of the impedance method to detect incipient amounts of damage, use only a low excitation voltage, and the ability to both excite and record structural response simultaneously with piezoelectric transducers. The use of piezoelectric materials as a self-sensing actuator also allows for additional techniques such as Lamb wave methods

to share the same transducers as those necessary for impedance method (Grisso 2011a).

2.1 Component Fabrication

In this study, the test structures are aluminum fatigue specimens constructed with typical Navy ship design details (Figure 1). Each of these medium sized specimens consists of a single stiffened plate at the location of an intersecting stiffened bulkhead, which provides stress concentration, and therefore crack initiation, sites. All connections are welded. The base plate and bulkhead material consist of 3/8 and 1/4 inch thick 5083-H116 aluminum, while the stiffeners are made of extruded 6061-T6 aluminum. Thick end plates are welded to the specimen to allow for placement of the plate in a tensile fatigue machine. Using the fatigue machine, different loading profiles are applied to groups of specimens in an effort to characterize the S/N curve for this type of plate intersection. The results from monitoring just one of these stiffened plate specimens are presented here. Sixteen strain gauges were applied to the specimen to assist in balancing the structure in the fatigue machine, as well as monitor the loading through the fatigue process.

2.2 Fatigue Testing and Data Acquisition

The specimen under investigation was secured and balanced in a 220 kip Instron machine. Fully reversed ($R = -1$), random amplitude loading was applied to the specimen. The average stress range of this loading was ± 2 ksi. Cycling was continued until the presence of a crack was detected. Generally, crack initiation would be considered a failure of the specimen. However, the crack was allowed to grow further in this case, and cycling continued until the crack propagated through one side of the plate.

As seen in Figure 1, four piezoelectric transducers were bonded to the surface of the base plate. Each transducer is a 0.5 inch diameter, 0.02 inch thick disc made of 851 material from APC, International and was bonded to the plate with Vishay Micro-Measurements M-Bond 200 adhesive. Each piezo disc is 6 inches down (Piezos 1 and

4) or up (Piezos 2 and 3) from the end plate fillet weld, and 2 inches left (Piezos 3 and 4) or right (Piezos 1 and 2) from the main plate stiffener fillet weld (Figure 1).

As the specimen was fatigued, the Instron machine was periodically paused to allow for impedance measurements to be recorded at specific cycle counts. Before the fatigue testing commenced, four baseline impedance signatures were generated for each of the piezoelectric transducers. Once fatigue testing began, two measurements were acquired from each of the piezos. These measurements were taken at the specific cycle counts presented in Table 1 as the test was paused.

Impedance measurements were acquired with a HP 4194A impedance analyzer controlled via a laptop running a custom LabView VI. Signatures were collected from 1,000 Hz to 200,980 Hz at 20 Hz intervals with medium integration and two averages. Only the real parts of the data were used for the analysis.

As the fatigue test progressed, a crack was visually observed at some point between 100 – 130 random amplitude loading blocks. Each random amplitude block is 5,000 fully-reversed fatigue cycles, so 100 random amplitude loading blocks equates to 500,000 fully reversed cycles. The crack was located in the heat-affected zone adjacent to the main plate butt weld. The crack started in the center of the plate, directly under the rathole in the stiffener. A rathole feature (seen in Figure 2) allows for the stiffener to be welded to the plate without having to grind the butt weld flush with the plate surface. In this specimen, the crack formed above the butt weld (closer to Piezos 1 and 3 in Figure 1). As previously mentioned, the test was not terminated due to the initiation of a crack, but allowed to continue. The crack initially grew through the plate thickness, and once through, proceeded along the butt weld towards the free edges of the test specimen. By the time the test was stopped at 136 random amplitude loading blocks (680,000 full cycles), a 1.5 inch crack was observed. By 276 random amplitude loading blocks (1,380,000 full cycles), the crack was approximately 1.5 inches from either edge of the specimen. Eventually, the crack extended completely to the edge (right side of Figure 1) in one direction between Piezos 1 and 2, and was less than an inch away from the other edge. The crack length description at each measurement cycle count is catalogued in Table 1, and Figure 3 displays the crack size on the back of the main plate labeled at specific cycle counts.

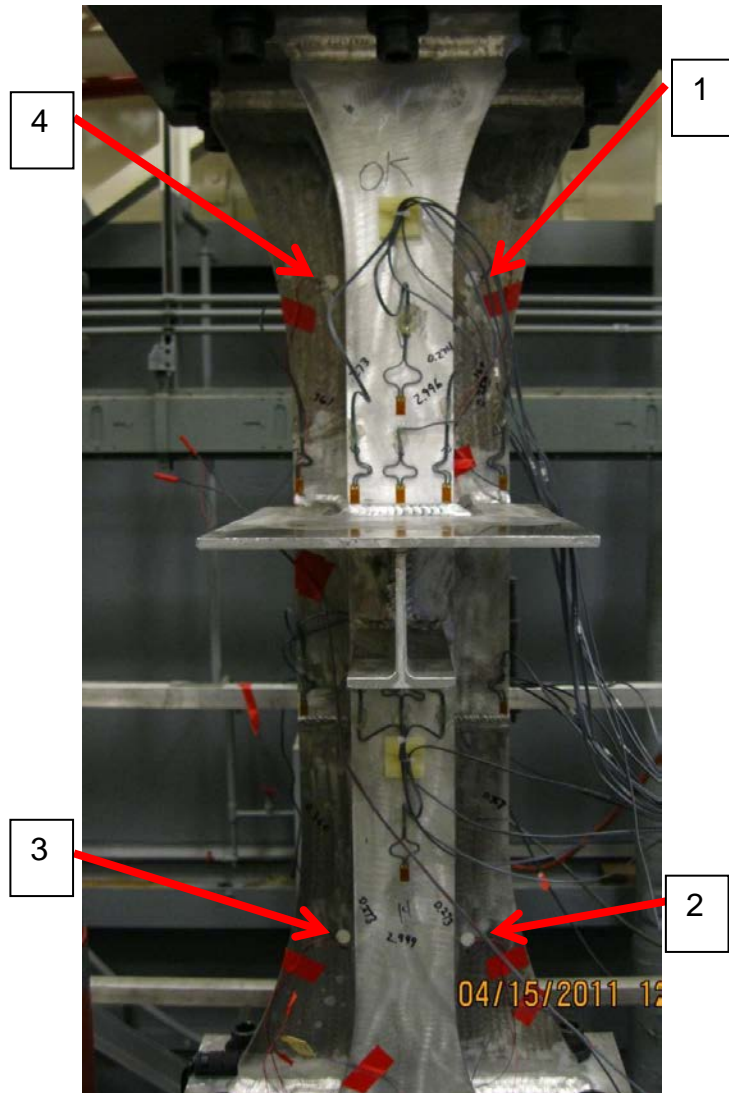


Figure 1. The front of an identical fatigue specimen is shown, and the four piezoelectric discs bonded to the plate are labeled.



Figure 2. The butt weld and rathole where crack initiation occurs are displayed.

Table 1. Measurement and damage condition descriptions.

RA Blocks	Specimen Temp	Visually Observed Damage
None	69° F	none
94	77° F	none observed
136	71° F	around 1.5" crack
156	75° F	growing
176	80° F	growing
196	88° F	growing
276	74° F	crack approx 1.5" from either edge
296	79° F	growing
308.7	79° F	crack extended through right edge of specimen (between PZTs 1&2), less than 1" from edge on other side

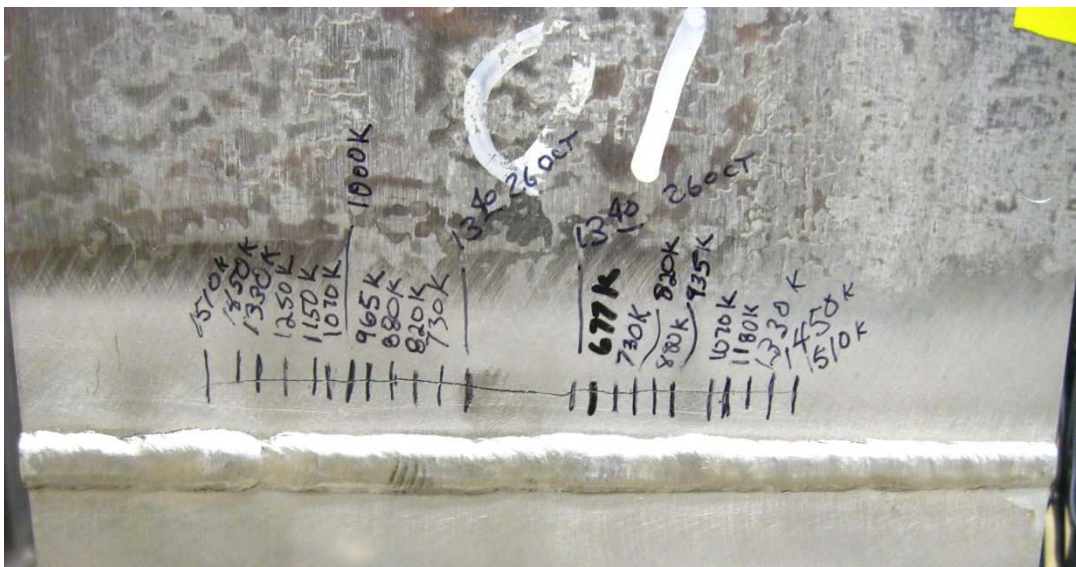


Figure 3. The crack growth is displayed on the back of the main plate. Note that the total, not random amplitude, cycle count is used in the markings.

2.3 Data Analysis

Figure 4 displays the real part for each of the acquired impedance signatures for Piezo 1 from 100 – 200 kHz. As displayed in Figure 4, the peaks of the impedance signature start to change and shift as fatigue and crack growth is accumulated in the specimen. The more the structure is damaged, the more the peaks shift from their original, or baseline, state. In general, impedance measurements for structural health monitoring purposes are taken over a range of frequencies from 10 kHz to 400 kHz (Park et al. 2003). This frequency range ensures the wavelength of excitation is smaller than the size of damage to be detected. Also, at these high frequencies, the method is generally insensitive to boundary condition changes, operational vibrations, or variations like mass loading. It is also important to note that the impedance method is a local detection method, not a global method. Therefore, the peaks displayed in the signatures of Figure 4 are not structural natural frequencies, but rather local modes. To analyze the change in impedance curves, a variation of the Root Mean Square Deviation (RMSD) damage metric is utilized to determine the amount of damage present. The RMSD method for finding the damage metric, M , can be described as

$$M = \sqrt{\sum_{i=1}^n \frac{[Re(Z_{i,1}) - Re(Z_{i,2})]^2}{[Re(Z_{i,1})]^2}}, \quad (1)$$

where $Z_{i,1}$ is the baseline, or healthy, impedance of the PZT, and $Z_{i,2}$ is the impedance used for comparison with the baseline measurement at frequency interval i . Figure 5 displays this damage metric in bar chart form for Piezo 1.

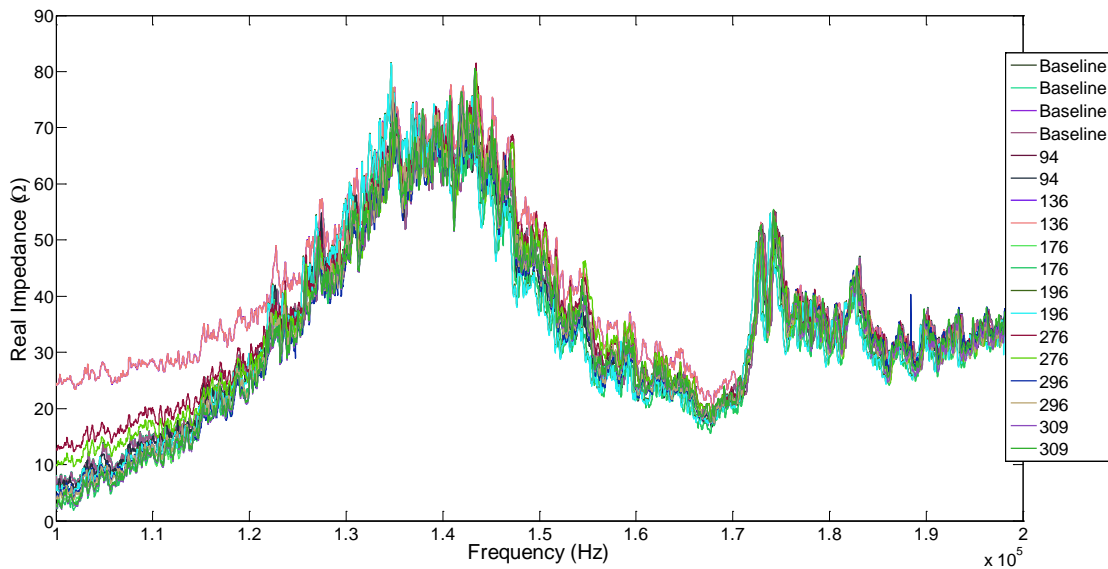


Figure 4. Real impedance is displayed for Piezo 1 from 100 – 200 kHz.

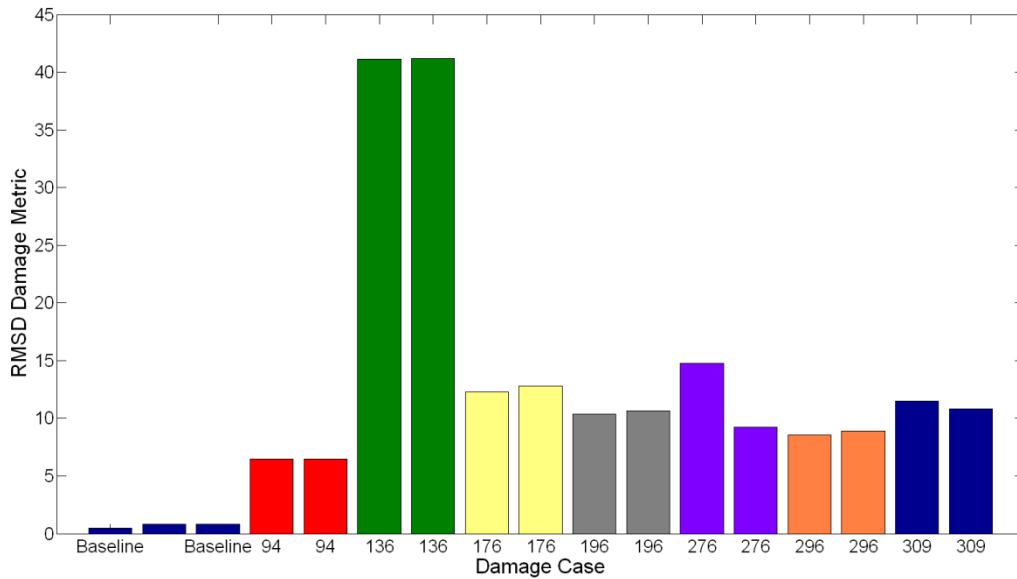


Figure 5. The RMSD damage metric displays the amount of change in each impedance signature to the first baseline measurement.

As noted earlier, four separate baseline signatures were acquired from each transducer for this specimen. The first of these baseline signatures is used as the undamaged case, or $Z_{i,1}$, for comparison to each of the other curves. In Figure 5, the

first three bars, labeled “Baseline” compare the remaining three baseline signatures (taken before fatigue testing) with the first baseline. The bars represent the values of M generated by the RMSD equation. Ideally, with no noise or variance in the data acquisition system or environment, the first three bars would be zero, thus indicating that each of the baseline measurements are identical. The rest of the bars in the chart correspond to the two measurements acquired at each of the fatigue levels described in Table 1 (ie “94” is the measurement taken after 94 random amplitude loading blocks) compared with the first baseline curve.

Analyzing Figure 5, we can easily see that, as expected, the three baseline values are close to zero and show little variation. This is a good indication that there is at least short term repeatability when acquiring measurements. Each of the remaining RMSD values show a large change from the baseline, indicating significant damage has occurred to the structure. The values are not very indicative of the quantity of damage (in this case, crack length) in the structure, but over a broad frequency range with a multitude of peaks, this result is not completely unexpected. Going back to Figure 4, it appears that the most consistent interaction between the piezo transducer and the base structure occurs at the higher end of the acquired frequency range. Figure 6 displays the real impedance signatures for Piezo 1 from 170 – 200 kHz.

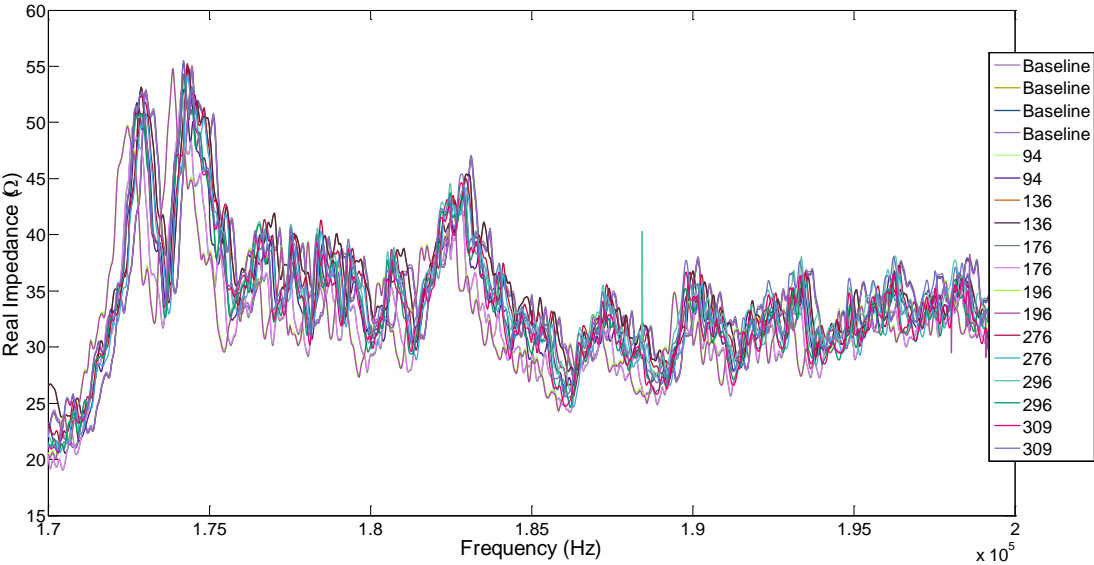


Figure 6. The real impedance is displayed for Piezo 1 from 170 – 200 kHz.

In Figure 6, we can get a much better indication of how the peaks of the impedance curves are shifting due to damage. Based on observing data over a broader frequency range, the peaks seen here appear to be more consistently interactive with the base structure. Figure 7 shows the RMSD values calculated from the signatures displayed in Figure 6.

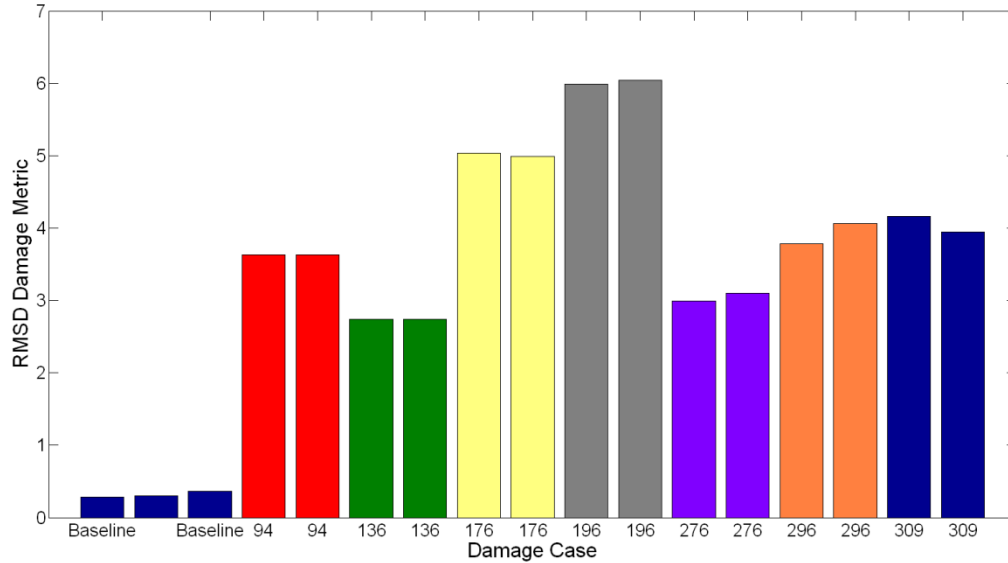


Figure 7. The RMSD damage metric values are shown for Piezo 1 from 170 – 200 kHz.

Figure 7 looks more indicative of what might be expected from a damage metric curve. Starting with the measurements taken after 94 random amplitude blocks, we see an increase in the amount of damage indicated through measurement 196, with the noted exception of cycle count 136. After 196 blocks, there appears to be a shift in the metric, but then another increasing trend is seen (corresponding to a growing crack).

Unfortunately, data was not acquired in large gap between 196 and 276 random amplitude loading blocks, which equates to 400,000 full cycles, so it is hard to say with any certainty what occurred between measurements to cause the shift. However, the crack was already almost completely through the structure by the time the 276 random amplitude data was taken, so between the dramatic change in crack length, as well as, the accumulated amount of fatigue, it is not unexpected to see changes in the signatures (new peaks appearing and other) that could ‘trick’ the damage metric into

appearing more similar to the baseline state than earlier damage metrics. The important thing to note is that we are easily indicating that damage is present. One could envision setting a threshold RMSD level at two for this frequency range simply alerting an end user to the presence of significant change if the threshold level is exceeded.

The other interesting phenomenon noted in Figure 7 is that damage is indicated after 94 random amplitude loading blocks, which occurs before damage was visually observed (between 100 – 130 blocks). There are two likely scenarios as to why this may be the case. The first possibility is that by 94 blocks, there actually was a small crack in the structure, but the crack went overlooked by the operators running the test. Detecting small cracks during a fatigue test is very much an art, so this theory is certainly not out of the realm of possibility.

The second scenario is that there was not actually a crack that could be visually detected in the structure, but that the impedance method was still able to detect significant change in the structure without the presence of an open crack. In many cases, the impedance method has been shown to be very sensitive to incipient amount of damage (Park *et al.* 2003). It is not uncommon for damage to be found before anything can be visually observed.

The detection of incipient damage actually correlates well with what was noted in another of these fatigue tests. As noted earlier, a number of these fatigue specimens were fabricated and tested in an effort to characterize S/N curves for these particular design details. In another of these tests, the specimen was instrumented with four piezoelectric transducers in the same manner as described in this test. However, in this case, Lamb wave propagations with an energy analysis damage detection technique were used as the structural health monitoring methods. Interestingly, the energy analysis for monitoring measured guided waves also indicated damage in the structure right before a crack was visually observed (Grisso 2011b). Unfortunately, in this test, there were no data sets collected between the baseline and 94 random amplitude blocks, so whether there was a precursor to damage indicated or just an unobserved crack will remain unknown.

Now that the data acquired from Piezo 1 has been analyzed, the measurements taken from the other transducers can also be investigated. In this specimen, the crack occurred above the main plate butt weld. However the damage was actually physically closer to Piezos 2 and 3. The real impedance signatures for Piezo 2 in the range of 170 – 200 kHz are shown in Figure 8.

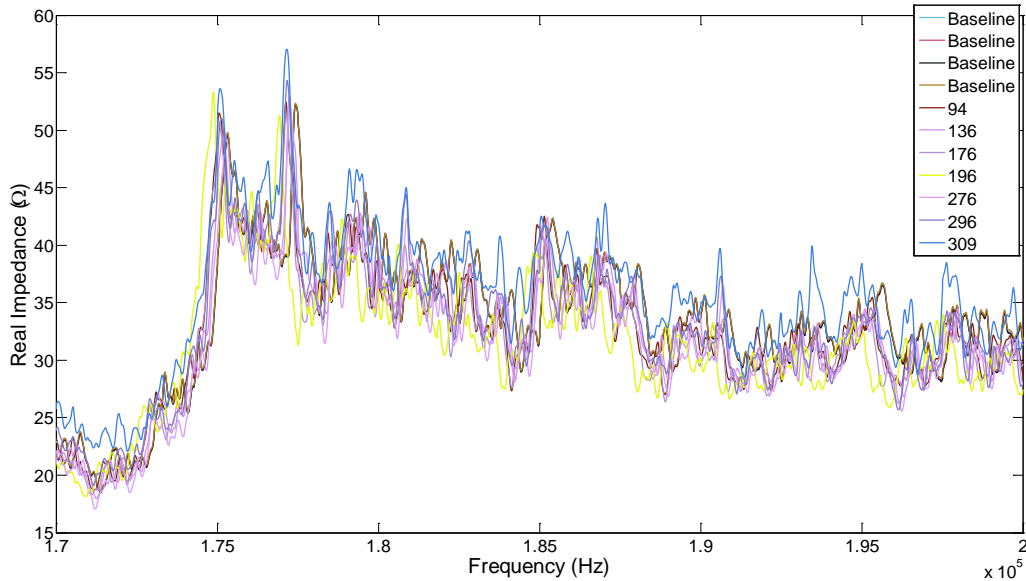


Figure 8. The real impedance is show for Piezo 2 from 170 – 200 kHz.

In Figure 8, the only one measurement (of the two collected) is shown for each of the fatigue cycle counts to allow for increased graph readability. The measurements at each fatigue level remained repeatable. Interestingly, the curves shown in Figure 8 are very similar to those seen in Figure 6 for Piezo 1. Even though the transducers are in locations remote from each other, the transducer/sensor interaction appears to be very similar. Figure 9, the RMSD values calculated from the curves of Figure 8, also confirms this result.

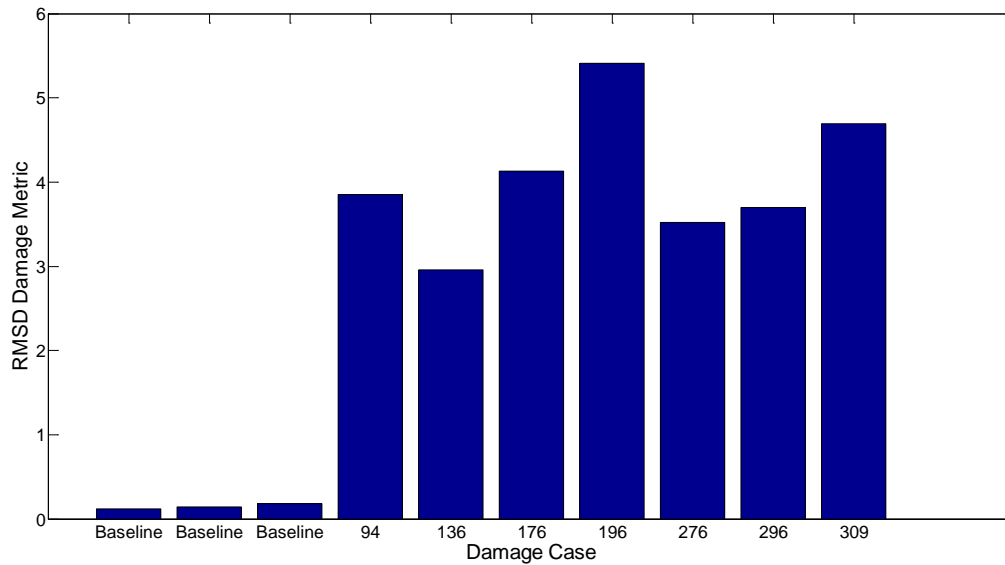


Figure 9. The RMSD damage metric values are shown for Piezo 2 from 170 – 200 kHz.

The same damage metric value trends seen in Figure 9 for Piezo 2 are seen as those in Figure 7 for Piezo 1. As with Figure 8, only one RMSD value is shown for each labeled fatigue cycle count. The similar damage detection results between transducers on opposite ends of the test structure leads to two conclusions. One, the two transducers are each able to detect the crack (and Piezo 2 can “see through” the butt weld to the crack). Two, the transducer bonding at either location were consistent at the beginning and throughout the test. In other words, the changes indicated in the RMSD values are unlikely to be due to changes in the transducer bonding conditions. To further back up these points, the impedance signatures and RMSD values for Piezo 3 are shown in Figure 10.

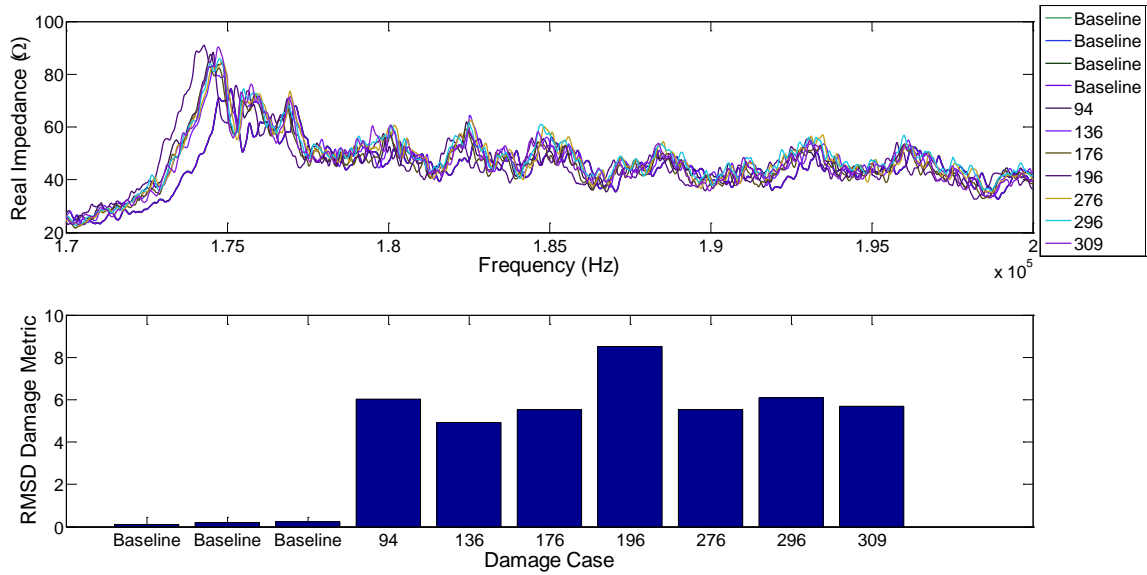


Figure 10. The real impedance (top) and RMSD damage metric values (bottom) are shown for Piezo 3 from 170 – 200 kHz.

As indicated in Figure 10, both the impedance signatures and RMSD values for Piezo 3 are similar to the corresponding figures for Piezos 1 and 2. Again, this result is a good indicator that actual structural changes are being detected as opposed to changes in bonding conditions, noise, or other external variables. Overall, the results from this chapter indicate that the impedance method is a suitable damage detection technique for realistic aluminum specimens undergoing fatigue.

3. Hardware Development

In the literature review, a number of citations were highlighted detailing various approaches to developing portable impedance SHM hardware. In the past, the principal investigator of this report had investigated developing custom hardware from the low-cost circuit and components such as digital signal processor boards. For this investigation, a prototype will instead be developed around the Analog Devices, Inc. AD5933 impedance chip.

3.1 Basic Evaluation Board Operation

The AD5933 impedance converter network analyzer is a small (0.26 x 0.22 x 0.07 inch) integrated circuit (IC) incorporating a frequency generator and a 12-bit, 1 MSPS (MHz) analog-to-digital converter (ADC) (Analog Devices 2011a). The chip can actuate and measure frequencies up to 100 kHz with a frequency resolution of less than 0.1 Hz. Impedance can be measured in the range of 1 k Ω to 10 M Ω . That range can be reduced to between 100 Ω to 1 k Ω with additional circuitry. The integrated circuit also contains an internal temperature sensor. Full details of the chip can be found in the technical data sheet provided by Analog Devices, Inc. (Analog Devices 2011a).

As a method to efficiently evaluate the usage and effectiveness of the AD5933 chip, Analog Devices has generated an evaluation board (EVAL AD5933EB) based around the chip (Analog Devices 2007). The evaluation board contains several components around the impedance chip that allow the user to control and program the chip via a graphical user interface, power the chip via USB cable from a computer or external power supply, and select from two system clocks (an internal chip RC oscillator or board 16 MHz crystal). Full details of the evaluation board components, layout, and operation can be found on the technical data sheet provided by Analog Devices (Analog Devices 2007). The evaluation board is seen in Figure 11.

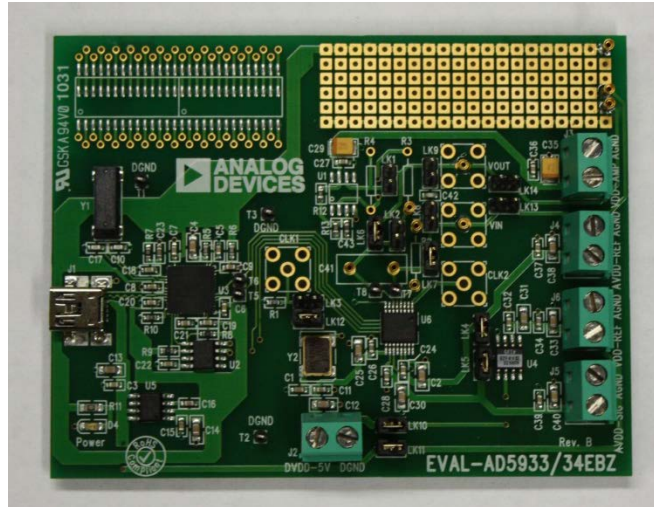


Figure 11. The AD5933 evaluation board.

Understanding how AD5933 EB and chip responds to basic measurements was the initial focus of this study. Using the AD5933 diagrams and manual, proper configuration and calibration of the board began. Once measurements of simple electrical components appeared correct from the board, the HP 4194A impedance analyzer was used to duplicate the results and act as a standard for correct measurement values.

After the evaluation board was properly configured, initialized, and calibrated, simple components (resistors, capacitors, etc.) were measured. An example of a basic component measurement can be seen in Figure 12 for a capacitor. As expected, the magnitude is decreasing linearly around a frequency of 10 kHz. Once familiarity with these basic components was established, simple circuits (resistors, capacitors, combinations of both in series, parallel, circuits, etc.) were also analyzed. With measurements from the evaluation board matching those of the impedance analyzer, it was time to move on to measuring a piezoelectric transducer.

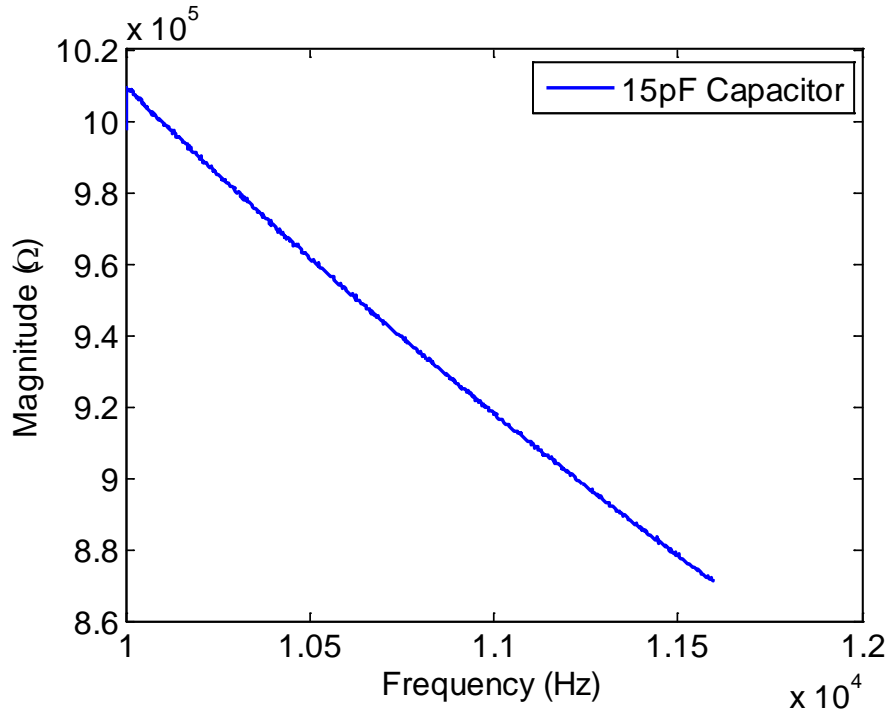


Figure 12. A 15pF capacitor is measured with the AD5933 evaluation board.

3.2 Evaluation Board Piezoelectric Testing

Utilizing the experience gained from measuring basic components and verifying results with a known standard, the AD5933 EB was attached to a piezoelectric transducer. In this case, a 0.5 inch diameter, 0.02 inch thick piezoelectric disc made of 851 material from APC, International was bonded to a small test plate with Vishay Micro-Measurements M-Bond 200 adhesive. The test structure consists of two 3x3x0.25 inch, 5083-H116 aluminum plates welded together with a butt joint. The test plate with three attached transducers is shown in Figure 13. For these experiments, the single piezo disc on the left of the plate is used.

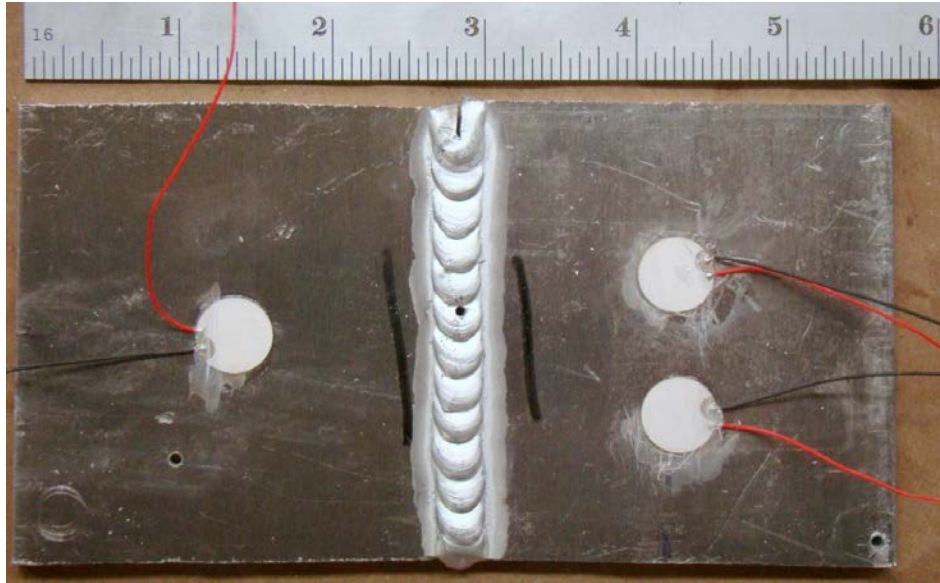


Figure 13. A small plate with a butt weld and three piezo discs is shown.

The specimen was first attached to the impedance analyzer, and signatures were collected from 10 – 40 kHz. The impedance magnitude is shown in Figure 14. For a simple comparison with the AD5933 data, a couple of peaks were chosen to view more closely. The two large peaks seen between 35 – 36 kHz are displayed in Figure 15.

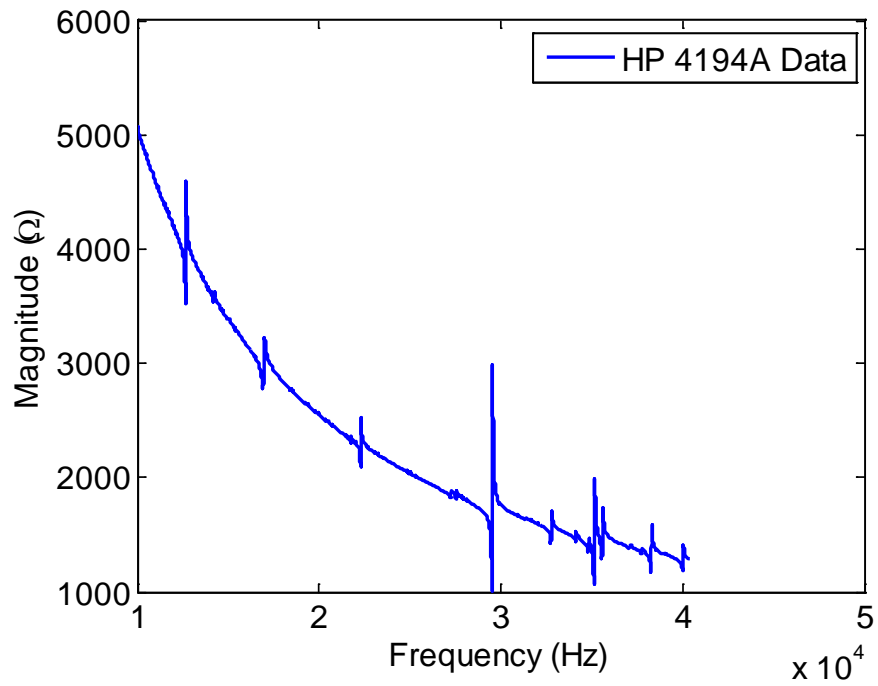


Figure 14. Impedance magnitude is shown as measured with the HP 4194A impedance analyzer from 10 – 41.98 kHz.

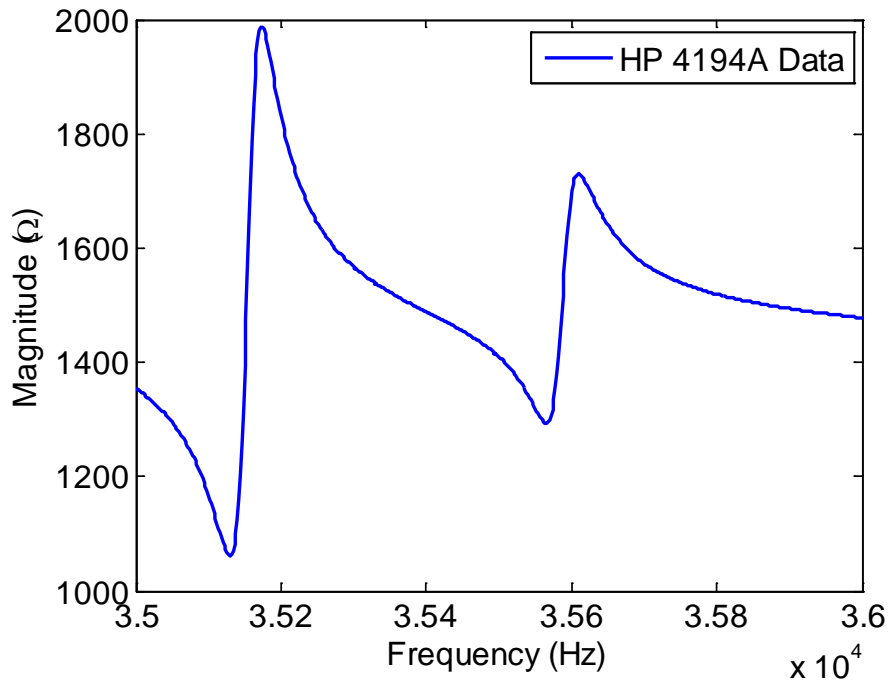


Figure 15. Impedance magnitude is shown as measured with the HP 4194A impedance analyzer from 35 – 36 kHz.

The specimen was then connected to the AD5933 evaluation board (Figure 16) to acquire duplicate measurements. As seen in Figure 17, the waveforms are identical in shape. The peak amplitudes are slightly different, and the mean of the evaluation board data is shifted. However, the peak frequency location and overall shape of the signature, which are the valuable pieces of data for structural health monitoring, are identical.

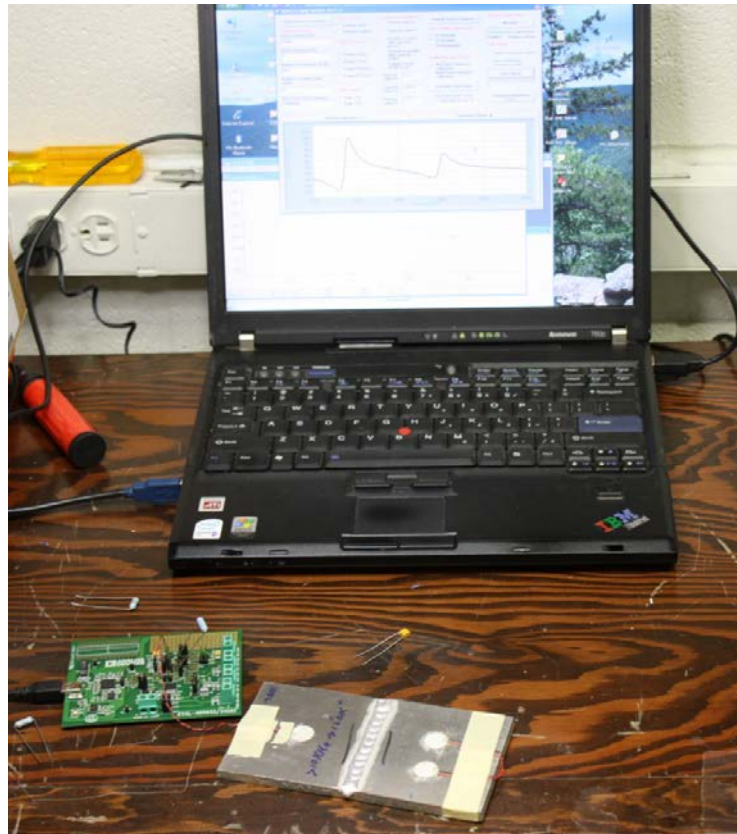


Figure 16. The test plate is connected to the AD5933 EB and controlled via a USB laptop connection.

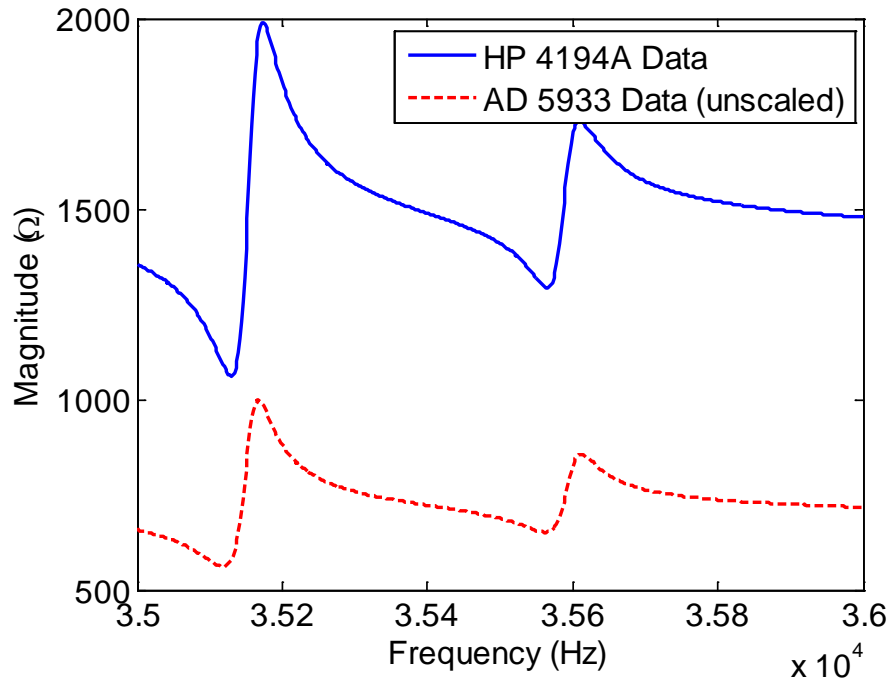


Figure 17. A comparison of HP 4914A and AD5933 impedance magnitude data from 35 – 36 kHz.

Overall, these tests reveal that the AD5933 evaluation board and chip can be confidently applied to measure impedance directly. With the impedance method, the accuracy (having the correct amplitude measurement) is not necessarily integral to the SHM process; only looking for changes in the waveform shape are required to find damage. However, in the following sections, steps will be identified to ensure that the measurements from the evaluation board more closely match those from impedance analyzer.

3.3 Evaluation Board Modifications

Before designing and fabricating an impedance measurement prototype based upon the AD5933 impedance chip, there are a couple of improvements that were made to the evaluation board. The board comes with a small section for adding custom components to the existing circuitry (top right of Figure 11). This prototyping area will be used for testing several components before deciding on the right hardware and configurations necessary for a SHM prototype.

One of the recommendations Analog Devices makes to improve high frequency measurements and overall impedance measurement quality is to add a small amplifier to the existing evaluation board circuitry. The amplifier chosen here is the Analog Devices 820A. The 820A is a single-supply input (from 5 V to 30 V) op amp useful for 12-bit to 14-bit data acquisition systems (Analog Devices 2011b). The AD5933 evaluation board with the AD 820A amplifier addition is shown in Figure 18.

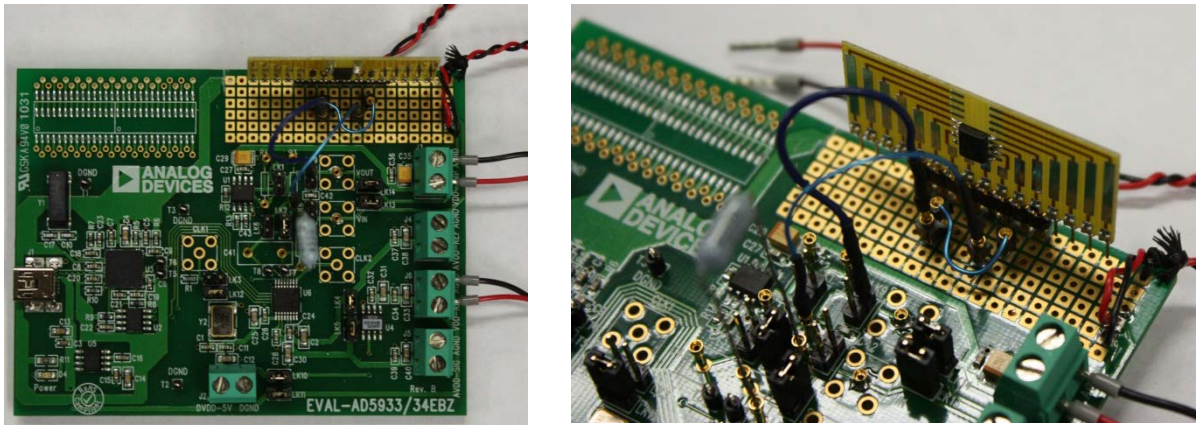


Figure 18. The modified evaluation board (left) is shown with a view of the amplifier (right)

The second, although very minor, alteration to the evaluation board is to simply add a 100 Ω resistor in series with the piezo disc being interrogated. As mentioned in the description the AD5933 chip, the lower limit of the impedance measurement range is too high for many piezoelectric applications. The extra resistor simply raises the overall impedance of the transducer to a range more easily measured with the impedance IC.

By adding an amplifier to the board and including a resistor in series with the transducer, a full structural health monitoring test could be completed. The details of this test are found in the following section along with the description of an appropriate test structure representative of a naval application.

3.4 Modified Board Health Monitoring Testing

To check the modifications to the AD5933 evaluation board, a test structure was identified to assess the damage detection capabilities of the board. The results were then compared side-by-side with the standard HP 4914A impedance analyzer. Unlike

previous sections in this chapter, damage was introduced to allow for a full health monitoring evaluation of the AD5933 impedance chip.

The structure used for these experiments starts with 6 x 3 foot, 0.25 inch thick piece of 5083-H116 aluminum. The base plate has two holes cut out of it to represent typical complexities (pipe through holes, etc.) seen in typical naval bulkhead designs. A ring of bolt holes surrounds each of the larger through holes. The location and size of these holes can be seen in Figure 19.

Two doublers, as detailed in Figure 20, are attached to the center of the plate with 36 one inch long SAE Grade 8 ¼-28 bolts, matching nuts, and top and bottom flat washers. Again, the doubler material is fabricated from 0.25 inch thick 5083-H116 aluminum. For this test, a 0.5 inch diameter, 0.02 inch thick piezoelectric disc made of 851 material from APC, International and was bonded to the plate with Vishay Micro-Measurements M-Bond 200 adhesive four inches below the bottom of the left doubler and nine inches from the left edge of the base plate. The assembled test structure is placed in end clamps for fixed-fixed boundary conditions and can be viewed in Figure 21.

To begin the experiment, a torque wrench was used to uniformly tighten each bolt to 70 in-lbs. Two baseline measurements were taken with both the HP 4194A impedance analyzer and the AD5933 evaluation board. In each case, data was acquired from 10,000 Hz to 41,980 Hz with a frequency resolution of 20 Hz.

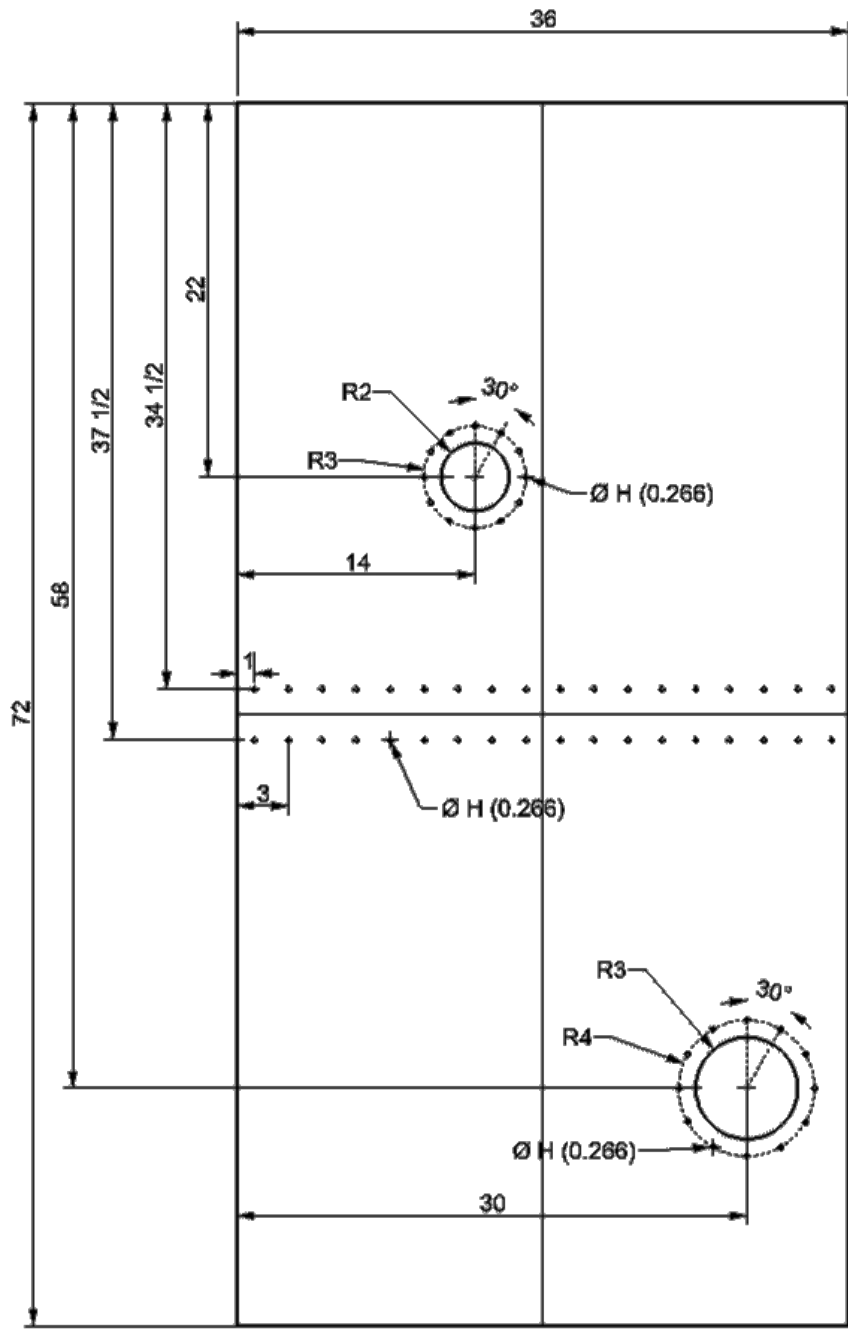


Figure 19. The base plate of the test structure. Dimensions are in inches unless otherwise specified.

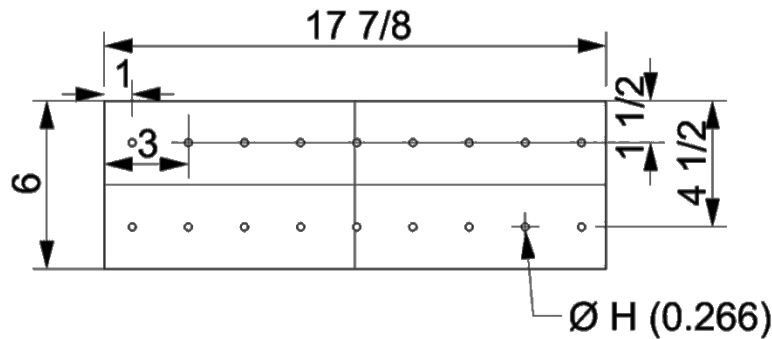


Figure 20. The dimensions (in inches) are shown for a plate doubler.



Figure 21. The base plate is placed in end clamps to supply fixed-fixed boundary conditions. The HP 4194A impedance analyzer is shown in the right of the picture.

As a source of repeatable damage, it was decided to loosen several of the bolts that attached the left doubler to the base plate. First, in the lower row of bolts on the left doubler, the second bolt from the left was completely loosened. This bolt is labeled as “Bolt A” in Figure 22. The AD5933 evaluation board and HP 4194A impedance analyzer were then both used recorded data from the Bolt A damage case. Next, the third bolt in the row, Bolt B, was completely loosened, and data was once again recorded from each device. When Bolt B was loosened, Bolt A was not retightened but remained loose. The process of loosening bolts and recording the data was repeated two more times for Bolts C and D, the next two bolts in the row, as see in Figure 22. All damage was cumulative.



Figure 22. The left doubler, piezo disc, and loosened bolt labels are displayed.

Analysis of the data proceeded very similarly to the steps outlined in Section 2.3. First, the real parts of the impedance are plotted for each of the baseline and damage cases. Second, the RMSD damage metric value, M , is calculated using Equation 1. The M values are then displayed in bar chart form to visualize the amount of change between each of the impedance signatures and the first baseline. Figure 23 displays the real impedance curves collected using the impedance analyzer and their resulting M values.

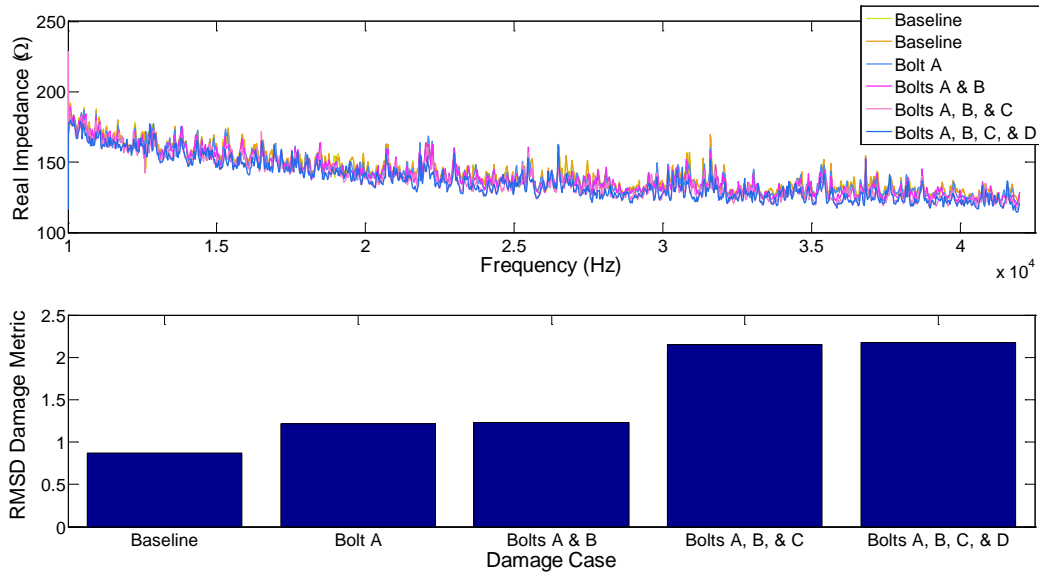


Figure 23. The real impedance (top) and RMSD damage metric (bottom) are shown from 10 – 41.98 kHz as measured by the HP 4194A impedance analyzer.

As Figure 23 shows, there are a large number of peaks in the chosen frequency range, which indicates there is good interaction between the transducer and host structure. The damage metric results in the bottom of the graph show an increase in damage metric. If we narrow down the selected frequency range, the RMSD values correlate well with the change in the structure. Figure 24 displays the impedance analyzer results from 20 – 30 kHz.

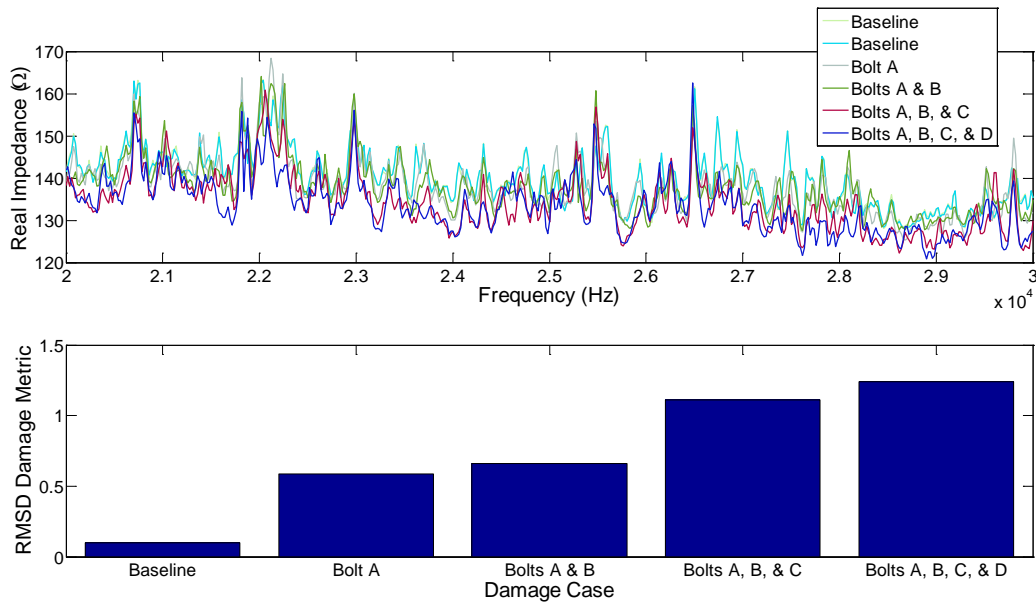


Figure 24. The real impedance (top) and RMSD damage metric (bottom) are shown from 20 – 30 kHz as measured by the HP 4194A impedance analyzer.

With an increased amount of damage accumulation in the structure, Figure 24 reveals the damage metric increases accordingly. The top plot in Figure 24 also clearly shows a good example of how the peaks in the impedance signature shift and change amplitude as the structure is damaged. With a standard set from the impedance analyzer of what measurements and results for this experiment should look like, the AD5933 evaluation board results are now compared. Figure 25 reveals the real impedance collected with the AD5933 and the calculated RMSD damage metric values.

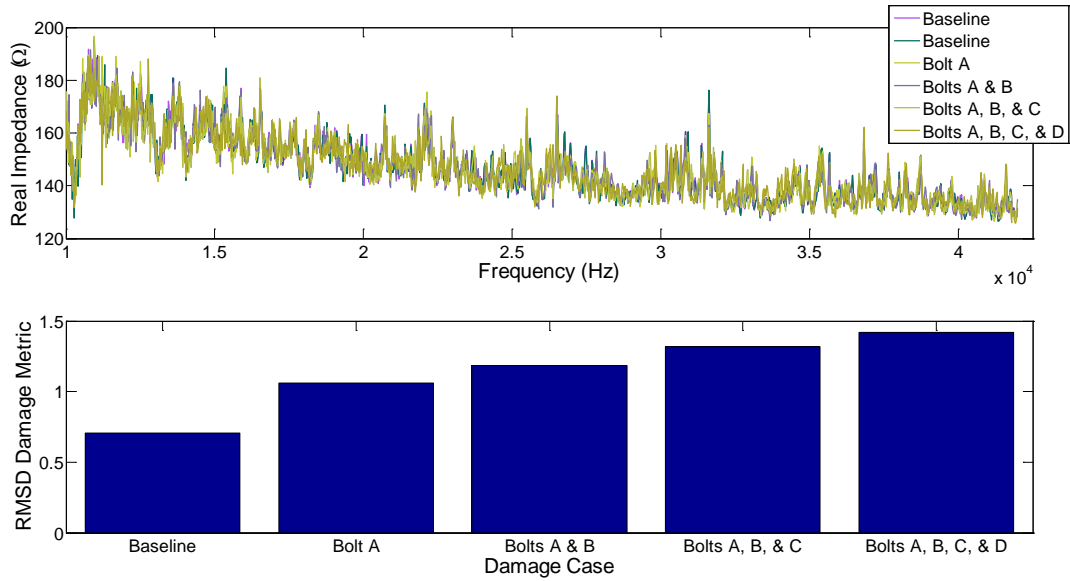


Figure 25. The real impedance (top) and RMSD damage metric (bottom) are shown from 10 – 41.98 kHz as measured by the AD5933 evaluation board.

The signatures measured with the AD5933 evaluation board and RMSD trends seen in Figure 25 correlate very well with their counterparts from the impedance analyzer displayed in Figure 23. Again, the damage metric rises appropriately as the quantity of loose bolts increases. Similarly to Figure 24, the frequency band of analysis is reduced and displayed in Figure 26 for the evaluation board.

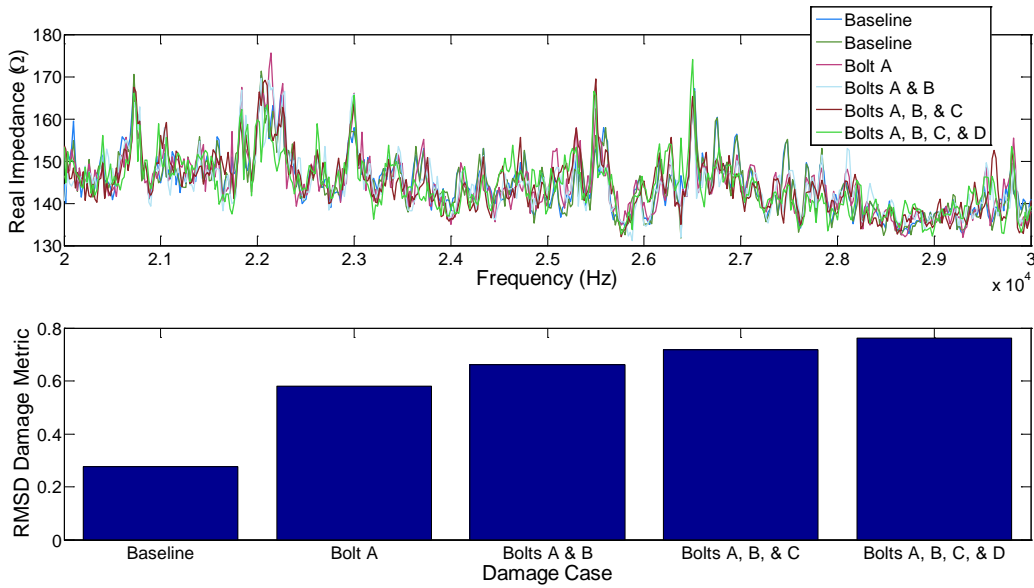


Figure 26. The real impedance (top) and RMSD damage metric (bottom) are shown from 20 – 30 kHz as measured by the AD5933 evaluation board.

As expected, Figure 26 and Figure 24 also correspond well to one another. These results are a very encouraging step in the development of impedance hardware using the AD5933 impedance chip. Results indicate that damage can be detected in a relatively complex structure using the AD5933 with accuracy approaching that of an impedance analyzer.

For one final check, one of the collected baselines from each of the data acquisition devices are displayed on the same graph. As Figure 27 reveals, the peaks captured with each device match very well with one another. The only discrepancy appears to be a slight drift (shift in the mean impedance) in the AD5933 signal near the beginning and ending frequencies. However, the captured frequency response content is unchanged due to this shifting.

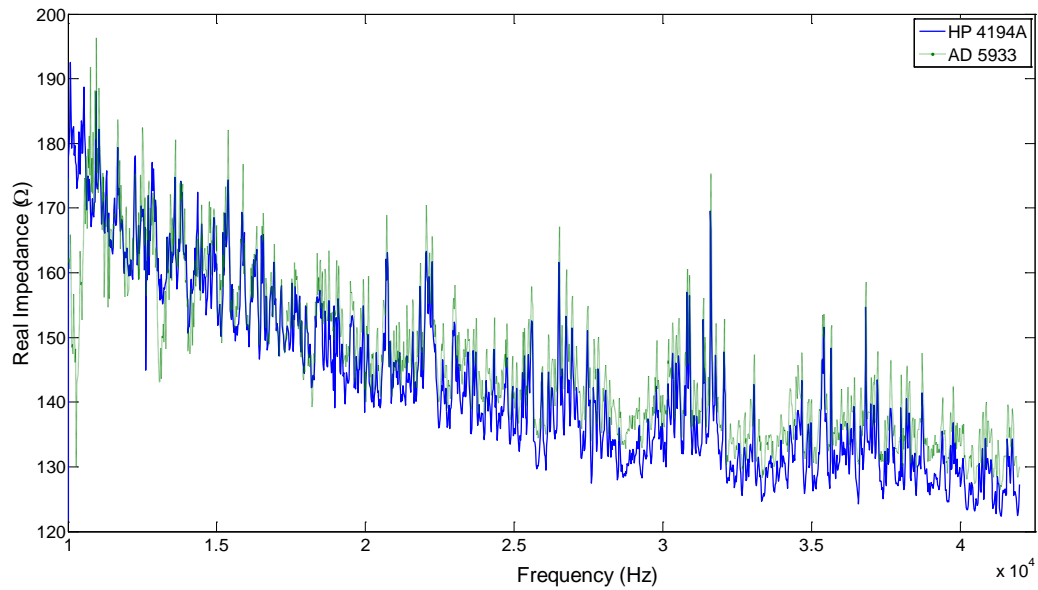


Figure 27. One baseline measurement is show for both the AD5933 evaluation board and the HP 4914A impedance analyzer from 10 – 41.98 kHz.

Reducing the frequency range, Figure 28 shows the peak matching in greater detail. The results of this chapter indicate that accurate measurements can be made with the impedance chip to the extent of being able to find damage. Steps will be taken in the prototype design outlined in the next chapter to reduce the mean impedance drift seen when comparing the AD5933 to the impedance analyzer.

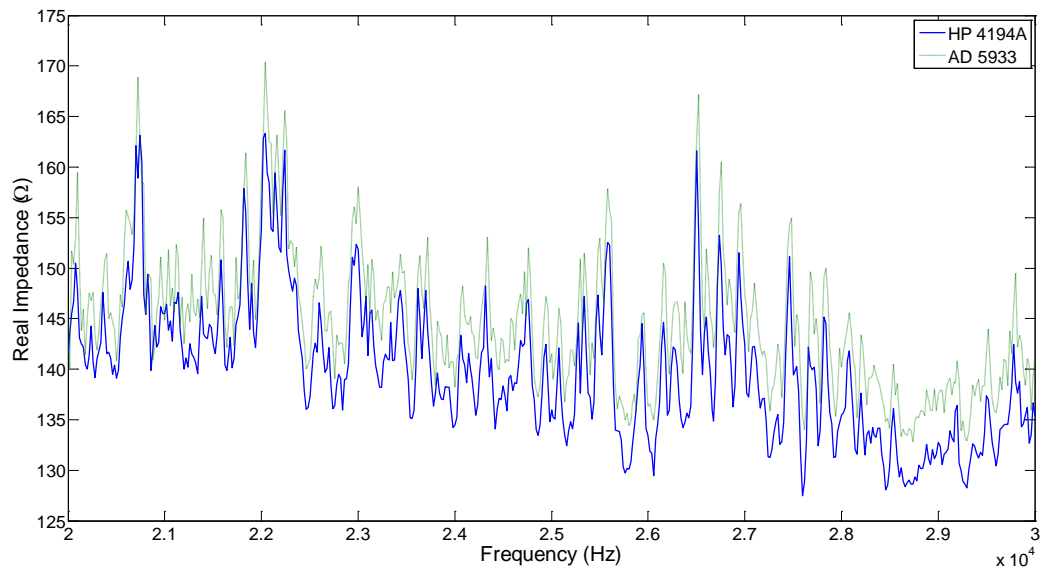


Figure 28. One baseline measurement is shown for both the AD5933 evaluation board and the HP 4914A impedance analyzer from 20 – 30 kHz.

4. Initial Prototype Design

The goal of this project is to develop impedance SHM hardware useful in both laboratory and field environments. While an impedance analyzer is useful in most laboratory settings, its bulky size and high cost are not suitable for most field applications. In the previous section, we have already determined that the AD5933 impedance chip is an acceptable alternative to impedance analyzers for SHM data acquisition. In this chapter, the first steps towards making the impedance chip more suitable for naval damage detection measurements will result in outlines for an initial prototype. Emphasis will specifically be placed on increasing the user-friendliness of the chip and conforming to the Navy standard of open architecture hardware and software.

4.1 Low Ohm Impedance Measurements

As mentioned in Section 3.1, the AD5933 IC can accurately measure impedance from 1 k Ω to 10 M Ω . It was also stated that, with additional circuitry, the measurement can be reduced to 100 Ω to 1 k Ω . Analog Devices has recently developed another evaluation board with the circuitry similar to the one mentioned above. The goal of this modified circuitry is to provide accurate impedance measurements, including low Ohms, up to several hundred kilohms while also optimizing the overall accuracy of the AD5933 IC. By incorporating two AD8606 op amps in the circuitry, the impedance measurement level can accurately be extended down to 10 Ω or less (Analog Devices 2011c).

Essentially, what this circuitry provides for impedance SHM measurements is eliminating the requirement of placing a resistor in series with the piezoelectric transducer. With the accurate measurement range of the AD5933 IC lowered, there is no further requirement to artificially raise the Ohms of the structure being interrogated. Before the prototype designs are completed, this new evaluation board from Analog Devices (CN0217) was evaluated to see if the modified circuitry does provide more accuracy in lower Ohm measurements. The CN0217 evaluation board is displayed in Figure 29.

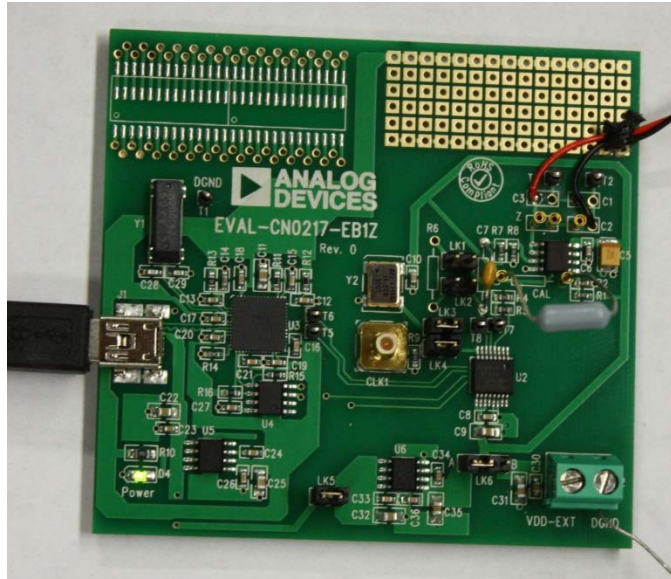


Figure 29. The Analog Devices CN0217 evaluation board.

To evaluate the performance of the new evaluation board, data is taken with both the CN0217 and HP 4194A impedance analyzer on the large aluminum plate described in the previous chapter and seen in Figure 21. The goal of this test is not to perform a SHM study, but rather to simply compare measurements taken with the CN0217 circuit to those of an impedance analyzer. As such, the bolt torque condition is irrelevant as long as the state remains unchanged between measurements between devices. Several measurements were taken on the transducer shown in Figure 22, which lies on the main plate four inches below the left doubler. Repeatability of the measurements was excellent for both data acquisition systems. Figure 30 displays measurements from each device over the entire acquisition band of 10 – 41.98 kHz. Only one curve is shown from either device to assist in the ease of viewing the figure.

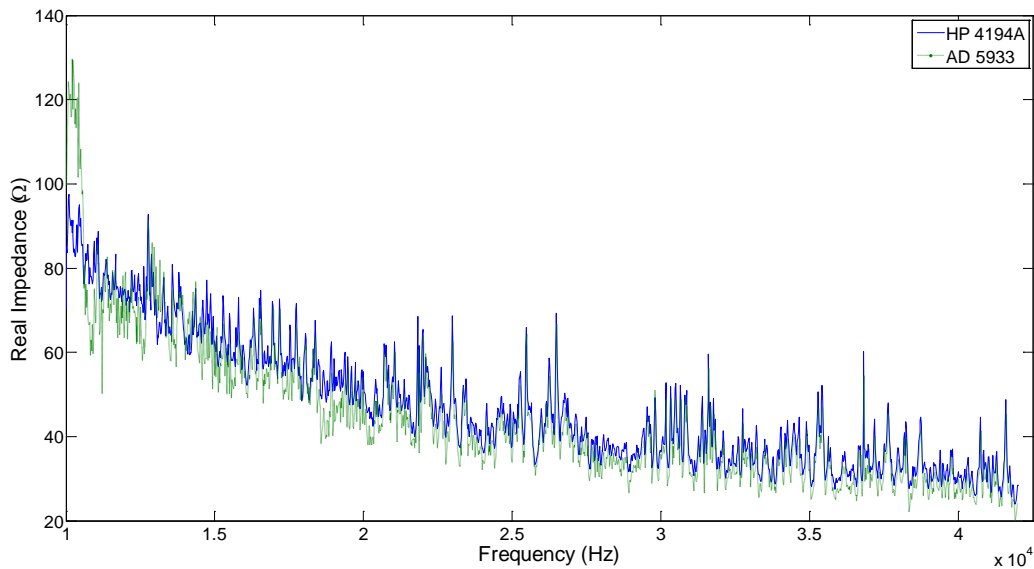


Figure 30. Real impedance signatures acquired from the CN0217 evaluation board and HP 4194A impedance analyzer are compared from 10 – 41.98 kHz.

As Figure 30 reveals, the only significant discrepancy between the two curves is the “hump” shown by the AD5933 data using the CN0217 circuit at the low end of the graph (under 11 kHz). However, this feature was present in the measurements taken with the generic evaluation board (Figure 27), and, as long as the low end inaccuracy remains consistent, is not a concern for SHM data. Remember, we are only interested in comparing curves to a baseline, not necessarily exactly matching measurements from an impedance analyzer. Narrowing the frequency range displayed in Figure 30, we can see just how well the peaks correlate (Figure 31).

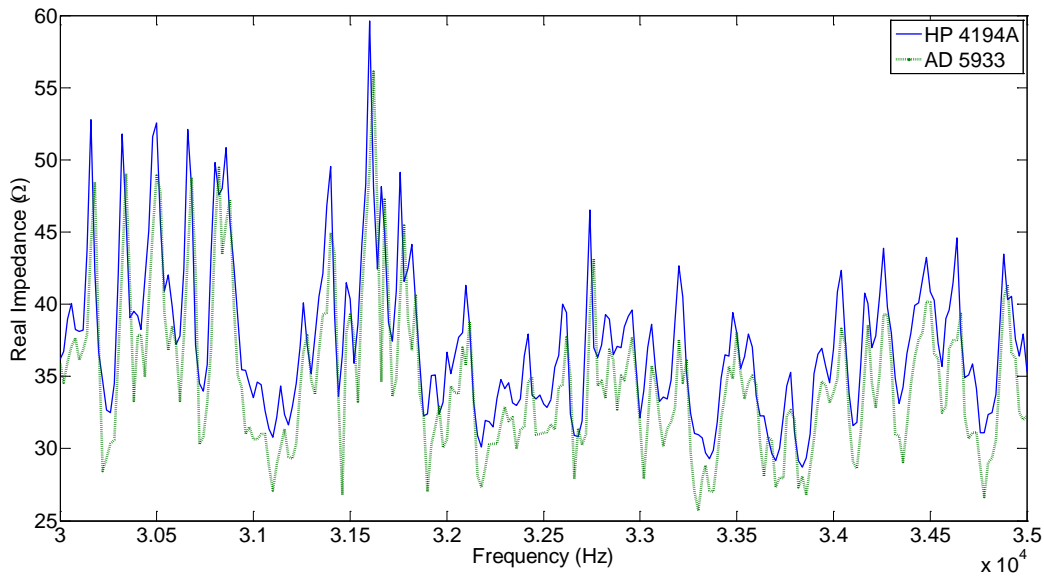


Figure 31. Real impedance signatures acquired from the CN0217 evaluation board and HP 4194A impedance analyzer are compared from 30 – 35 kHz.

All the peaks seen by the impedance analyzer are captured accurately by the AD5933 with improved circuitry in Figure 31. This plot shows dramatic improvement over the previous evaluation board (Figure 27 and Figure 28) where the curve started to significantly drift at the higher end of our measurement range. Zooming in to just a few peaks, Figure 32 displays an even more narrow frequency range.

Peaks are captured with much greater accuracy using the CN0217 circuit. The drift at higher frequencies seen in Figure 27 and Figure 28 are significantly upgraded with the new circuitry. Low impedance measurement accuracy is also greatly improved, eliminating the need for an additional resistor to artificially increase transducer impedance. Overall, results indicate that, in general, impedance measurements are much more accurate with the new circuitry. The CN0217 circuit paired with the AD5933 chip appears to be a logical choice to design the first prototype.

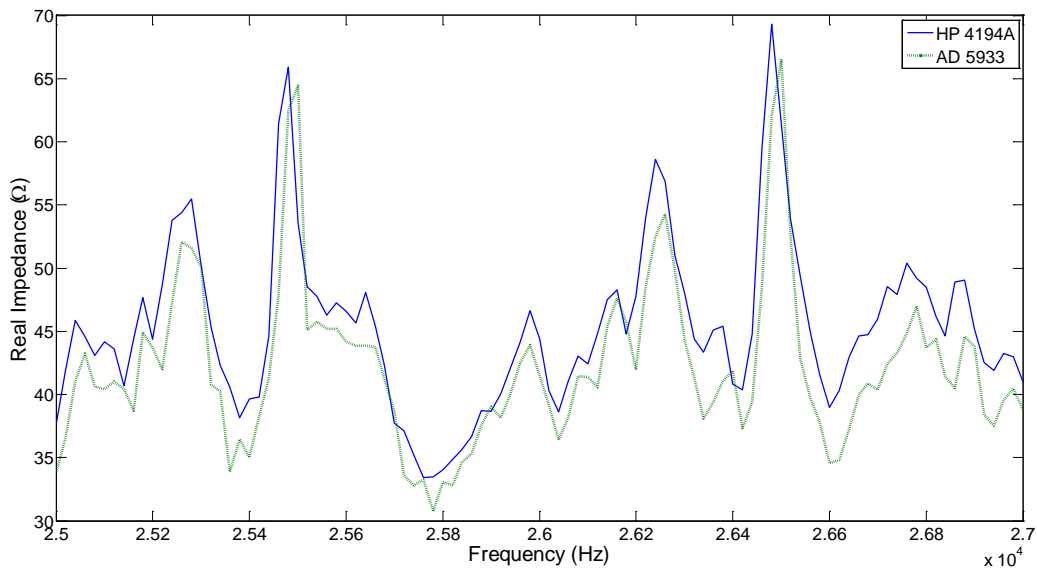


Figure 32. Real impedance signatures acquired from the CN0217 evaluation board and HP 4194A impedance analyzer are compared from 25 – 27 kHz.

4.2 Prototype Concept

With the results seen in the previous section, a SHM prototype starting with the AD5933 impedance chip including the CN0217 measurement enhancement circuit seems like a logical place to start the circuit design.

4.2.1 Design and Verification Process

There are a number of steps required to obtain a piece of impedance hardware for use specifically with naval structures. Each of the steps below will assist in designing the most robust piece of hardware possible.

1. Design a circuit based upon experimental results from this study (including the corresponding required operational software)
2. Convert the design block diagram to a printed circuit board (PCB) layout
3. Fabricate the PCB
4. Experimentally evaluate the initial PCB prototype
5. Document limitations of the prototype and desired improvements and modifications

6. Redesign the circuit and corresponding PCB layout; fabricate modified PCB
7. Extensively evaluate the final design on a number of realistic naval test structures

The first step in completing this process is described in the following section.

4.2.2 Initial Design

The first step of designing an impedance prototype for naval applications is to layout the required components in a circuit block diagram. Results from previous testing indicated that the additional CN0217 circuitry provides the most accurate impedance measurements from piezoelectric transducers. Starting with the AD5933 chip as a base, and adding the CN0217 circuitry, the initial prototype block diagram can be seen in Figure 33.

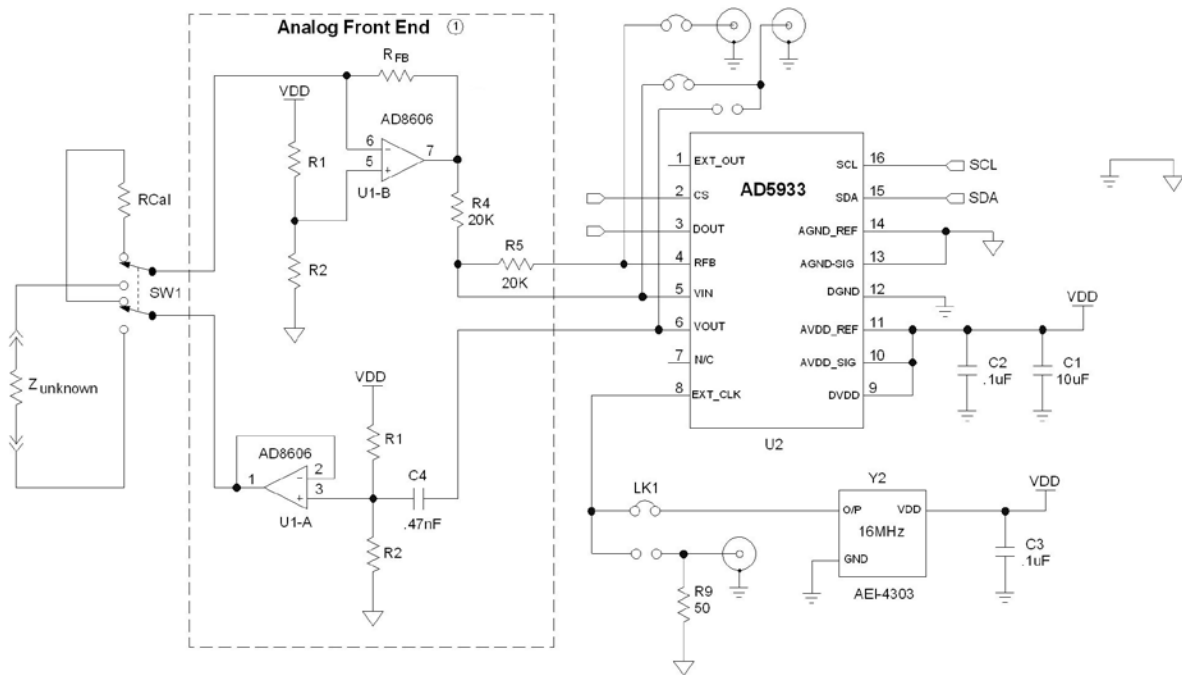


Figure 33. An initial circuit block diagram is shown based upon the AD5933 chip and CN0217 circuit.

The AD5933 impedance IC is the main component seen in Figure 33. As discussed in prior sections, the AD5933 already contains integrated functionality to provide an excitation signal to a structure and record the response using a built-in ADC. Impedance measurements can be accurately captured up to a frequency of 100 kHz. With a consistent power supply to the AD5933 IC, the device registers can be programmed externally to set the desired acquisition parameters (frequency range, frequency resolution, gain, and calibration setting).

An analog front end is displayed in Figure 33. Based upon the CN0217 circuitry, the main function of the analog front end is to interface with the piezoelectric transducer. By placing the front end between the test structure and the impedance IC, the electrical load is isolated from the vital AD5933. The other benefit of the analog front in is to greatly improve the measurement accuracy for impedance values under 500 Ω (typical of many piezo transducers used for impedance SHM and those shown in this study).

The main components in the analog front end are two AD8606 operational amplifiers. These amplifiers, along with other basic components (resistors and capacitors) allow the AD5933 to measure impedances as low as 10 Ω . The circuit design also allows provides stability and accuracy in acquiring impedance measurements.

On the left of Figure 33, a switch, $SW1$, is seen between R_{cal} and $Z_{unknown}$. This switch is a crucial addition to the circuit design and allows for the accommodation of different types of piezoelectric transducers to be interrogated. Part of the basic operation of the AD5933 involves a calibration of the device based upon a known resistance value of similar range to the transducer being tested. In this case, $Z_{unknown}$ is the impedance of the piezoelectric transducer bonded to our structure of interest. R_{cal} is the known resistor used for device calibration purposes. The switch allows for straightforward calibration and can be externally controlled. The plan is to include a bank of resistors corresponding to typical transducer and structural impedances. Multiple calibration options allows for easy accommodation of different sensors without having to manually change parts of the prototype hardware (which can lead to measurement errors and inaccuracies). While the hardware will be capable of monitoring different types of transducers, the initial prototype will focus on measuring a

single transducer at a time. Future developments could include an integrated multiplexer to monitor multiple transducers simultaneously. Impedance hardware is capable of monitoring transducers over a distance several hundred feet, but monitoring transducers over only a few feet is generally preferable to reduce the influence of the wire connector impedance in the measurements.

Besides the circuit design, the second major component of this initial prototype is software design. As mentioned, the prototype will need to be controlled externally for this initial design. External control will allow for ease in programming device registers, including such options as changing the desired frequency measurement range. External control also allows for data to be easily downloaded to a connected computer for analysis. Future designs may include onboard data processing and storage.

The software for this initial prototype is a graphical user interface (GUI) made from National Instruments LabView software. A LabView Virtual Instrument (VI) allows for a straightforward interface between a laptop or other computer and the prototype utilizing a USB connection. The software developed here will provide several improvements over using one of the evaluation boards for data collection. One change will be to modify the way data is collected and stored. Over broad frequency range measurements, the evaluation board records require a user to manually append files post data collection. This software will automatically store files in a user-friendly format. The acquisition calibration process can also be automated to avoid manually switching between a calibration component (resistor) and the device under test. This automation would also allow for the selection of the correct calibration resistor. The final change will be integrated phase calculations to automatically find and save the real part of the impedance signature necessary for damage detection computations.

Unfortunately, at the time of writing this report, the prototype circuit was never able to be fabricated. Hence, the circuit block diagram and corresponding developed software were unable to be tested and validated. An underdeveloped prototype has also curtailed the remaining hardware development phases outlined in Section 4.2.1.

5. Conclusions and Recommendations

While the initial goal of completely designing, fabricating, and validating custom impedance hardware may have been slightly ambitious for the scope of this work, discoveries resulting from this research are still quite valuable.

5.1 Brief Report Summary

Many structural health monitoring investigations are performed on simplistic test specimens with simulated damage in ideal laboratory conditions. Taking these basic research results and expanding them to complex physical specimens with real damage mechanisms can often be the limiting factor in applying damage detection techniques to real world components. Results from Chapter Two provide some necessary middle ground between simple tests and a deployment of SHM on actual Navy assets. Results revealed the ability of the impedance method to detect cracking in a complex structure typical of real ship designs. An actual crack in the structure was formed while the specimen was subjected to realistic (random amplitude) fatigue loading.

Knowing that the impedance method holds great promise for detecting real damage in ship structures, the initial investigations into miniaturized impedance hardware for use in naval settings were detailed in Chapter Three. An evaluation board is used to understand the operation of an impedance chip. Knowledge from these initial tests is used to undertake a full SHM evaluation on a large plate structure. Damage detection results compare favorably to identical data acquired with an impedance analyzer.

Chapter Four used the insight gained on impedance integrated circuit operation to design an initial impedance-based SHM prototype. A new circuit is employed to increase measurement accuracy. Software adds valuable functionality to make the prototype as user friendly as possible. The overall hardware design provides tangible improvements when compared with using an evaluation board setup in an identical capacity.

5.2 Contributions

A few key contributions from this research should be noted. The use of impedance-based techniques to actual fatigue cracking on a complex naval component is a significant result. As previously mentioned, most SHM assessments use simulated damage or are performed on simplistic laboratory test specimens. Testing here represents some of the most complex testing and verification of the impedance method for use specifically on a naval application.

The first known and documented use of CN0217 circuitry for use in impedance SHM applications is outlined in this report. This circuitry should provide the highest accuracy for impedance measurements of small piezoelectric transducers. Additionally, while data acquisition with the AD5933 evaluation boards can be somewhat tedious, we do now possess operational hardware which can be used for initial laboratory or field evaluations of Navy assets until either our prototype is completed or open architecture impedance hardware is available for purchase.

5.3 Future Work Recommendations

With additional interest expressed in this project, future work and research would be fairly straightforward. A basic path forward is already outlined in Section 4.2.1. The initial block diagram for an impedance hardware prototype is complete. The next steps would be to layout and fabricate a PCB. Evaluation and validation of the manufactured hardware would direct the remaining research and development necessary to facilitate a fully developed damage detection device compatible with ship structures and systems. Provided there is future interest in this project, an initial prototype could be fabricated reasonably quickly and inexpensively.

Acknowledgements

The author is grateful to the Ship Structure Committee (SSC) for taking interest in structural health monitoring for ship structures and providing a pathway for this research to develop. Chao Lin of the Department of Transportation is especially acknowledged for chairing the Project Technical Committee (PTC), organizing the meetings, and keeping the project on track. I am grateful to the rest of the PTC for providing valuable feedback and suggestions throughout the duration of this project.

Funding for this SSC project was provided by David Qualley (NAVSEA, SEA 05) utilizing Systems Engineering Technical Authority (SETA) research project funds.

The author wishes to acknowledge financial support provided by Dr. Paul Hess of Code 331 at the Office of Naval Research (ONR) for the fatigue specimen test in Chapter Two. Fatigue specimen design and coordination of fabrication were conducted at the Naval Surface Warfare Center, Carderock Division (NSWCCD) by Edward Devine (NSWCCD, Code 654). Fatigue testing of the specimen was performed by Dr. David Kihl and Nancy Adler of NSWCCD, Code 653.

Dr. Ignacio Perez of Code 332 at ONR provided funding for the design and fabrication of the large aluminum plate used for experimentation in Chapter Three.

The author is grateful to Jesus Rosario (NSWCCD, Code 653) for his efforts in configuring the evaluation board and designing the prototype circuitry described in Chapters Three and Four.

Finally, I wish to thank Jeff Mercier (NSWCCD, Code 653) for providing managerial support of this project and allowing the technical research to advance.

References

ABS, 2003. "Guide for Hull Condition Monitoring Systems (Pub #73)."

Adams, D. E., 2007. *Health Monitoring of Structural Materials and Components: Methods with Applications*, John Wiley & Sons Inc., Hoboken, NJ.

Analog Devices, Inc., 2007. "EVAL-AD5933EB: Evaluation Board for the 1 MSPS 12-Bit Impedance Converter Network Analyzer Data Sheet."

Analog Devices, Inc., 2011a. "AD5933: 1 MSPS, 12-Bit Impedance Converter, Network Analyzer Data Sheet (Rev D, 12/2011)."

Analog Devices, Inc., 2011b. "AD820: Single-Supply, Rail-to-Rail, Low Power, FET-Input Op Amp Data Sheet (Rev H, 03/2011)."

Analog Devices, Inc., 2011c. "Analog Devices Circuit Note: High Accuracy Impedance Measurements Using 12-Bit Impedance Converters (CN0217 Rev 0)."

Bhalla, S., Gupta, A., Bansal, S. and Garg, T. 2009. "Ultra Low Cost Adaptations of Electro-Mechanical Impedance Technique for Structural Health Monitoring," *Journal of Intelligent Material Systems and Structures*, Vol. 20, No. 8, pp. 991-999.

Doebling, S. W., Farrar, C. R., and Prime, M. B., 1998. "A Summary Review of Vibration-Based Damage Identification Methods," *The Shock and Vibration Digest*, Vol. 30, No. 2, pp. 91-105.

Doherty, J. E., 1987. "Nondestructive Evaluation," Chapter 12 in: Kobayashi, A. S. (Edt.), *Handbook on Experimental Mechanics*, Prentice-Hall, Inc., Englewood Cliffs, NJ.

Farrar, C. R., and Worden, K. 2007. "An introduction to structural health monitoring," *Philosophical Transactions of the Royal Society A*, Vol. 365, pp. 303–315.

Giurgiutiu, V. and Xu, B., 2004. "Development of a field-portable small-size impedance analyzer for structural health monitoring using the electromechanical impedance technique," Proceedings of SPIE's 11th Annual International Symposium on Smart Structures and Materials, March 14-18, San Diego, CA, Vol. 5391, pp. 774-785.

Grisso, B. L., 2004. "Considerations of the Impedance Method, Wave Propagation, and Wireless Systems for Structural Health Monitoring," MS Thesis, Virginia Polytechnic Institute and State University, Blacksburg, VA,
<http://scholar.lib.vt.edu/theses/available/etd-09142004-151951/>.

Grisso, B. L., Martin, L. A., and Inman, D. J., 2005. "A Wireless Active Sensing System for Impedance-based Structural Health Monitoring," Proceedings of the 23rd International Modal Analysis Conference (IMAC XXIII), January 31-February 3, Orlando, FL.

Grisso, B. L., Kim, J., Farmer, J. R., Ha, D. S., and Inman, D. J., 2007. "Autonomous Impedance-based SHM Utilizing Harvested Energy" Proceedings of the 6th International Workshop on Structural Health Monitoring, September 11-13, Stanford, CA, pp. 1373-1380.

Grisso, B. L., 2007. "Advancing Autonomous Structural Health Monitoring," Ph.D. Dissertation, Virginia Polytechnic Institute and State University, Blacksburg, VA, <http://scholar.lib.vt.edu/theses/available/etd-12062007-105329/>

Grisso, B. L. and Inman, D. J., 2008. "Autonomous Hardware Development for Impedance-based Structural Health Monitoring," *Smart Structures and Systems*, Vol. 4, No. 3, pp. 305-318.

Grisso, B. L., Kim, J., Ha, D. S., and Inman, D. J., 2008. "Sensor Diagnostics for Autonomous Digital Structural Health Monitoring Systems," Proceedings of the 26th International Modal Analysis Conference (IMAC XXVI), February 4-7, Orlando, FL.

Grisso, B. L., Salvino, L. W., Singh, G., Singh, G, Tansel, I. N., 2011a. "A comparison of impedance and Lamb wave SHM techniques for monitoring structural integrity of and through welded joints," Proceedings of SPIE Volume 7984.

Grisso, B. L., Park, G., Salvino, L. W., and Farrar, C. R., 2011b. "Structural Damage Identification in Stiffened Plate Fatigue Specimens Using Piezoelectric Active Sensing," Proceedings of the 8th International Workshop on Structural Health Monitoring, September 13-15, Stanford, CA, pp. 1683-1690.

Hess, P. E. 2007., "Structural Health Monitoring for High-Speed Naval Ships," Proceedings of the 6th International Workshop on Structural Health Monitoring, Sept. 11-13, Stanford, CA, pp. 3-15.

Inman, D. J., Farrar, C. R., Lopes, Jr., V., and Steffen, Jr., V., 2005. *Damage Prognosis: For Aerospace, Civil and Mechanical Systems*, John Wiley & Sons, Ltd., Chichester, UK.

Kim, J., Grisso, B. L., Ha, D. S., and Inman, D. J., 2007a. "A system-on-board approach for impedance-based structural health monitoring," Proceedings of SPIE's 14th International Symposium on Smart Structures and Materials, March 18-22, San Diego, CA.

Kim, J., Grisso, B. L., Ha, D. S., and Inman, D. J., 2007b. "All-Digital Low-Power Structural Health Monitoring Systems," IEEE Conference on Technology for Homeland Security, Woburn, MA, May 16-17.

Kim, J., Grisso, B. L., Ha, D. S., and Inman, D. J., 2007c. "Digital Wideband Excitation Technique for Impedance-Based Structural Health Monitoring Systems," IEEE International Symposium on Circuits and Systems, May 27-30, New Orleans, LA.

Kim, J. K., Zhou, D., Ha, D. S., and Inman, D. J., 2009. "A structural health monitoring system for self-repairing," Proc. SPIE 7295, Health Monitoring of Structural and Biological Systems.

Kou, S., 2003. *Welding Metallurgy*, John Wiley and Sons, Inc., Hoboken, NJ.

Liang, C., Sun, F. P., and Rogers, C. A., 1994a. "Coupled Electromechanical Analysis of Adaptive Material System – Determination of Actuator Power Consumption and System Energy Transfer," *Journal of Intelligent Material Systems and Structures*, Vol. 5, pp. 12-20.

Liang, C., Sun, F. P., and Rogers, C. A., 1994b. "An Impedance Method for Dynamic Analysis of Active Material System," *Journal of Vibration and Acoustics*, Vol. 116, pp. 121–128.

Mascarenas, D. L., Todd, M. D., Park, G., and Farrar, C. R., 2006. "A miniaturized electromechanical impedance-based node for the wireless interrogation of structural health," Proceedings of SPIE's 11th International Symposium on NDE for Health Monitoring and Diagnostics, February 26-March 2, San Diego, CA, Vol. 6177.

Min, J., Park, S., Yun, C.-B., and Song, B., 2010. "Development of a low-cost multifunctional wireless impedance sensor node," *Smart Structures and Systems*, Vol. 6, No. 5-6, pp. 698-709.

Overly, T. G. S., Park, G., Farrar, C. R., and Allemang, R. J., 2007a. "Compact Hardware Development for SHM and Sensor Diagnostics using Admittance Measurements," Proceedings of the 25th International Modal Analysis Conference (IMAC XXV), February 19-22, Orlando, FL.

Overly, T. G. S., Park, G., and Farrar, C. R., 2007b. "Development of Impedance-Based Wireless Active-Sensor Node for Structural Health Monitoring," Proceedings of the 6th International Workshop on Structural Health Monitoring, September 11-13, Stanford, CA, pp. 1660-1667.

Panigrahi, R., Bhalla, S., and Gupta, A. 2010. "A Low-Cost Variant of Electro-Mechanical Impedance (EMI) Technique for Structural Health Monitoring," *Experimental Techniques*, Vol. 34, No. 2, pp. 25–29.

Park, G., Sohn, H., Farrar, C. R., and Inman, D. J., 2003. "Overview of Piezoelectric Impedance-Based Health Monitoring and Path Forward," *The Shock and Vibration Digest*, Vol. 35, Issue 6, pp. 451-463.

Park, G., and Inman, D. J., 2007. "Structural health monitoring using piezoelectric impedance measurements" *Philosophical Transactions of the Royal Society A*, Vol. 365, pp. 373-392.

Park, S., Grisso, B. L., Inman, D. J., and Yun C.-B., 2007. "MFC-Based Structural Health Monitoring using a Miniaturized Impedance Measuring Chip for Corrosion Detection," *Research in Nondestructive Evaluation*, Vol. 18, No. 2, pp. 139-150.

Park, S., Shin, H., and Yun, C.-B., 2009. "Wireless impedance sensor nodes for functions of structural damage identification and sensor self-diagnostics," *Smart Materials and Structures*, Vol. 18, No. 5, pp. 1-11.

Peairs, D. M., Park, G., and Inman, D. J., 2004. "Improving Accessibility of the Impedance-Based Structural Health Monitoring Method," *Journal of Intelligent Material Systems and Structures*, Vol. 15, No. 2, pp. 129-139.

Quinn, W., Angove, P., Buckley, J., Barrett, J., and Kelly, G., 2011, "Design and performance analysis of an embedded wireless sensor for monitoring concrete curing and structural health," *Journal of Civil Structural Health Monitoring*, Vol. 1, No. 1-2, pp. 47-59.

Quinn, W., Kelly, G., and Barrett, J., 2012. "Development of an embedded wireless sensing system for the monitoring of concrete," *Structural Health Monitoring*, Vol. 11, No. 4, pp. 381-392.

Salvino, L. W. and Brady, T. F., 2007. "Hull Structure Monitoring for High-Speed Naval Ships," Proceedings of the 6th International Workshop on Structural Health Monitoring, Sept. 11-13, Stanford, CA, pp. 1465-1472.

Shankar, K., Wu, W., 2002. "Effect of welding and weld repair on crack propagation behaviour in aluminium alloy 5083 plates," *Materials & Design*, Vol. 23, No. 2, pp. 201-208.

Swartz, R. A., Zimmerman, A. T., Lynch, J. P., Rosario, J., Brady, T. F., Salvino, L. W., and Law, K. H., 2010. "Hybrid wireless hull monitoring system for naval combat vessels," *Structure and Infrastructure Engineering: Maintenance, Management, Life-Cycle Design and Performance*, Vol. 6, No. 3, pp. 1-18.

Taylor, S. G., Farinhold, K. M., Park, G., Todd, M. D., and Farrar, C. R., 2010. "Multi-Scale Wireless Sensor Node for Health Monitoring of Civil Infrastructure and Mechanical Systems," *Smart Structures and Systems*, Vol. 6, No. 5-6, pp. 661-673.

Wang, S., Zhao, Z., and You, C. 2010. "0.18 μm CMOS integrated circuit design for impedance-based structural health monitoring," *IET Circuits, Devices & Systems*, Vol. 4, No. 3, pp. 227-238.

Xu, B. and Giurgiutiu, V., 2006. "Development of DSP-based electromechanical (E/M) impedance analyzer for active structural health monitoring," Proceedings of SPIE's 13th International Symposium on Smart Structures and Materials, February 26-March 2, San Diego, CA, Vol. 6174.

Zhou, D., Kong, N., Ha, D. S., and Inman, D. J., 2010a. "A self-powered wireless sensor node for structural health monitoring", Proc. SPIE 7650, Health Monitoring of Structural and Biological Systems.

Zhou, D., Ha, D. S., and Inman, D. J., 2010b. "Ultra low-power active wireless sensor for structural health monitoring," *Smart Structures and Systems*, Vol. 6, No. 5-6, pp. 675-687.

SHIP STRUCTURE COMMITTEE LIAISON MEMBERS

LIAISON MEMBERS

American Society of Naval Engineers	Captain Dennis K. Kruse (USN Ret.)
Bath Iron Works	Mr. Steve Tarpay
Colorado School of Mines	Dr. Stephen Liu
Edison Welding Institute	Mr. Rich Green
International Maritime Organization	Mr. Igor Ponomarev
Int'l Ship and Offshore Structure Congress	Dr. Alaa Mansour
INTERTANKO	Mr. Dragos Rauta
Massachusetts Institute of Technology	
Memorial University of Newfoundland	Dr. M. R. Haddara
National Cargo Bureau	Captain Jim McNamara
National Transportation Safety Board - OMS	Dr. Jack Spencer
Office of Naval Research	Dr. Yapa Rajapaksie
Oil Companies International Maritime Forum	Mr. Phillip Murphy
Samsung Heavy Industries, Inc.	Dr. Satish Kumar
United States Coast Guard Academy	Commander Kurt Colella
United States Merchant Marine Academy	William Caliendo / Peter Web
United States Naval Academy	Dr. Ramswar Bhattacharyya
University of British Columbia	Dr. S. Calisal
University of California Berkeley	Dr. Robert Bea
Univ. of Houston - Composites Eng & Appl.	
University of Maryland	Dr. Bilal Ayyub
University of Michigan	Dr. Michael Bernitsas
Virginia Polytechnic and State Institute	Dr. Alan Brown
Webb Institute	Prof. Roger Compton

RECENT SHIP STRUCTURE COMMITTEE PUBLICATIONS

Ship Structure Committee Publications on the Web - All reports from SSC 1 to current are available to be downloaded from the Ship Structure Committee Web Site at URL:

<http://www.shipstructure.org>

SSC 445 – SSC 393 are available on the SSC CD-ROM Library. Visit the National Technical Information Service (NTIS) Web Site for ordering hard copies of all SSC research reports at

URL: <http://www.ntis.gov>

SSC Report Number	Report Bibliography
SSC 467	Incorporation of Residual Stress Effects in a Plasticity and Ductile Fracture Model for Reliability Assessment of Aluminum Ship Structures Hayden, M.J; Gao, X.; Zhou, J.; Joyce J.A. 2013
SSC 466	Mean Stress Assessment in Fatigue Analysis and Design Yuen, B.K.; Koko, T.S.; Polezhayeva, H.; Jiang, L. 2013
SSC 465	Predictive Modeling Impact of Ice on Ship and Offshore Structures Bueno A. 2012
SSC 464	Design and Detailing for High Speed Aluminum Vessels Design Guide and Training Mish, Wh Jr., Lynch T., Hesse E., Kulis J., Wilde J., Snyder Z., Ruiz F. 2012
SSC 463	Marine Composites NDE, Inspection Techniques for Marine Composite Construction Greene, E 2012
SSC 462	Review of Current Practices of Fracture Repair Procedures for Ship Structures Wang, G, Khoo, E., ABS Corporate Technology 2012
SSC 461	Structural Challenges Faced By Arctic Ships, Kendrick A., Daley C. 2011
SSC 460	Effect of Welded Properties on Aluminum Structures, Sensharma P., Collette M., Harrington J. 2011
SSC 459	Reliability-Based Performance Assessment of Damaged Ships, Sun F., Pu Y., Chan H., Dow R.S., Shahid M., Das P.K. 2011
SSC 458	Exact Mapping of Residual Stress in Ship Hull Structures by Use of Neutron Diffraction Das. S. Kenno S. 2009
SSC 457	Investigation of Plastic Limit States for Design of Ship Hull Structures, Daley C., Hermanski G. 2009
SSC 456	Buckling Collapse Testing on Friction Stir Welded Aluminum Stiffened Plate Structures, Paik J.K. 2009
SSC 455	Feasibility, Conceptual Design and Optimization of a Large Composite Hybrid Hull, Braun D., Pejicic M. 2008